



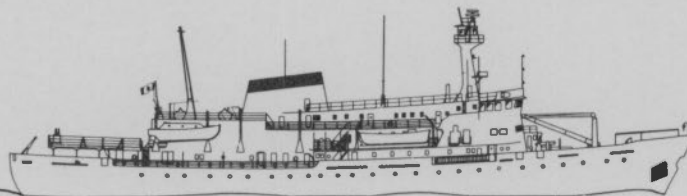
Energy, Mines and
Resources

Energie, Mines et
Ressources

**BEDFORD INSTITUTE
OF OCEANOGRAPHY**

**INSTITUT OCÉANOGRAPHIQUE
DE BEDFORD**

**GEOTECHNICAL ANALYSIS
OF
LABRADOR SHELF SEDIMENTS
AND THE
INFLUENCE OF ICE CONTACT PROCESSES**



Canada

This document was produced
by scanning the original publication.

Ce document est le produit d'une
numérisation par balayage
de la publication originale.

Geotechnical Analysis of Labrador Shelf Sediments
and the Influence of Ice Contact Processes

by

Armand J. Silva¹

Kathleen A. Dadey¹

Heiner W. Josenhans²

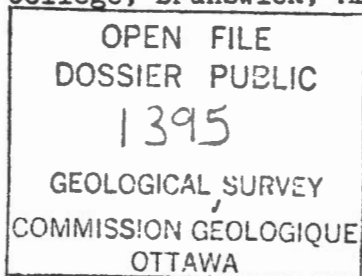
Edward P. Laine³

October, 1985

¹University of Rhode Island, Kingston, RI

²Bedford Institute of Oceanography, Dartmouth, Nova Scotia

³Present address: Bowdoin College, Brunswick, ME (Formerly at URI)



ABSTRACT

The report describes the basic geotechnical characteristics of the Labrador Shelf (Quaternary) sediments complicated by the interaction of ice with the seafloor. This investigation integrates geophysical and geological studies with geotechnical data to understand the influence of ice contact processes on sediment characteristics and to gain further insight into sediment history.

Three sedimentary units have been identified on the Labrador Shelf. Unit 3b, the Upper Till, is overconsolidated in shallow water near the ice sheet perimeter, due to the action of ice grounding. In deeper water this unit has not experienced significant loading from ice contact. The Hudson Strait Till (Unit 3c) also did not experience appreciable ice loading.

Most of Unit 4, a pro- and post-glacial marine sediment, is normally consolidated with no ice loading. There is evidence of loading of some strata which is attributed to iceberg scouring. This evidence indicates that scouring increases shear strength and decreases water content in sediments of this type.

We conclude that the sediments of the Labrador Shelf attributed to the last glaciation, i.e. units 3b, 4, and 5, have never experienced significant consolidating stresses due to loads imposed by thick ice sheets. The moderate amounts of overconsolidation in the upper till (Unit 3b) are attributed to partial ice loading developed in a situation in which the ice mass was primarily hydrostatically supported.

Table of Contents

	<u>Page</u>
Introduction.....	1
Geological Evolution.....	2
Sampling, Testing and Analysis Methods.....	5
Summary of Properties.....	8
Analysis and Discussion.....	11
Conclusions.....	16
Acknowledgements.....	17
Appendix A: Tabulations of Core Properties and Measurements.....	54
Appendix B: Consolidation Test Plots.....	67
Appendix C: Strain-energy Method for Preconsolidation Stress.....	78

Introduction

This report is a summary of a cooperative research effort by the Bedford Institute of Oceanography (BIO) and the University of Rhode Island, Marine Geomechanics Laboratory (URI/MGL). The goals of the program were to determine the basic geotechnical characteristics of Labrador shelf sediments and integrate the geophysical, geological and geotechnical properties in order to better understand the sedimentary processes and influence of ice contact on sediment characteristics. Results from CSS Hudson cruises 82-054, 83-030 and 84-035 along the Labrador shelf from Hamilton Bank (approximately 54°N) to Frobisher Bay (approximately 62°N; see Figure 1) are discussed.

This report presents the results of a geotechnical testing and analysis program carried out on sediments deposited on the Labrador shelf during the last glacial and post glacial periods. Although there were a limited number of samples available for testing, the careful selection of sample sites based on an extensive acoustic stratigraphic framework allows extrapolation of these results over a large area. The report includes a summary of the lateral distribution of physical characteristics and glacial history of the Labrador shelf sediments and integrates these with the geotechnical data.

The aim of this investigation is to characterize these deposits with respect to their properties and behavior, particularly the stress history and consolidation behavior. Other analyses also include vane shear strength, water content, bulk density, grain size and Atterberg limits. In

addition, lithology of the coarse fraction ($>63\mu\text{m}$) and percent calcium carbonate were determined for several of the cores.

Three unlithified Quaternary sedimentary units were tested during the course of the program. They have been affected by a number of different processes. Most significant are those associated with glaciers and glacial processes such as ice grounding and loading, and scour of deposits by icebergs. These processes are reflected in the geotechnical properties. The consolidation behavior and shear strength may be directly related to the action of the ice. Considerable insight into the depositional setting and subsequent modification of these deposits is gained through integration, analysis, and interpretation of the geological and geotechnical data.

General Geological Evolution

An extensive data base composed of medium and high resolution seismics (Fig. 2) was used to map the lateral distribution of nine acoustic stratigraphic units on the Labrador Shelf (Fig. 3; Josenhans et al., 1986). Core locations are shown in Figure 4. The data show a succession of superimposed tills, most of which exist over the entire shelf and extend to a depth of 500-600 m at the outer shelf break (Figs. 5 and 6). The upper till, designated as Unit 3b, is laterally restricted to the saddles and marginal trough, indicating deposition during less extensive glaciation. Summary profiles for Unit 3b are shown in Figs. 7, 8 and 9. Overlying the upper till is a conformable succession of stratified pro-glacial and post-glacial sediments herein designated as Unit 4. These drape (mimic) the underlying surface and in the deep basins are overlain by ponded muds

designated as Unit 5a. Physical property profiles are given in Figs. 7 through 13 and 16 through 19. At the entrance to Hudson Strait a late glacial readvance deposited another till (Unit 3c, see Fig. 10) above the conformable pro-glacial/post-glacial sediments.

The interpretation of the acoustic stratigraphic units is supported by visual, textural, geotechnical, paleontological, geochemical, and ^{14}C data. One complete deglacial cycle comprising the upper till (Unit 3b) and overlying post-glacial sequence (Units 4 and 5) was sampled and analyzed over broad areas of the shelf. In all cases this detailed ground truthing confirms and compliments the acoustic interpretations. The older till (Unit 3a), although exposed on the bank edges, was too consolidated and/or bouldery to allow adequate sampling with the available techniques - piston and gravity cores, and bottom grabs.

According to Josenhans et al. (1986), the style of glaciation indicates significant erosion as the glaciers advanced over the shelf, particularly in the marginal trough and saddles. This resulted in the development of smooth unconformities between the tills and a lack of stratified inter-till sediments. The geotechnical analyses described in this report show little to no true overconsolidation, suggesting that deposition of the youngest till occurred only during the retreat phase of the glacier when the ice was largely hydrostatically supported. Since till deposition occurs during ice retreat, the lateral extent of the upper till does not necessarily define the size of the advancing ice; it may have overlapped the banks without leaving any evidence. However, since previously deposited tills are clearly recognized on the bank tops, we conclude that the last glaciation,

represented by Unit 3b was less laterally extensive than earlier one(s) represented by Unit 3a.

Subglacial meltout and deposition of glaciomarine sediments beneath the ice sheet, which deposited Unit 3b, was limited or absent. Limestone fragments which only could have been ice rafted from northern sources are found immediately above this till, at the base of the stratified proglacial/post-glacial sediments. It appears that once the ice sheet which traversed the Labrador mainland began to float and calve it retreated without depositing significant amounts of stratified sediments. The lack of deposition from this ice sheet is probably a result of the resistant nature of the underlying crystalline bedrock which did not yield significant amounts of englacial material. In contrast, the large volume of glaciomarine silt (Unit 4) which is attributed to the Hudson Strait ice margin is likely derived from easily eroded limestone bedrock.

Deposition of the stratified sediments of Unit 4 was restricted to the deep saddles and marginal trough where low energy bottom currents and fiord-like sedimentation prevailed. At approximately 8000 years B.P., bottom current strength increased significantly. The period of low current velocities during deposition of Unit 4 is attributed to an ice barrier (margin) in Hudson Strait which physically blocked the Canadian and Labrador Currents and provided a limestone source. Truncation and erosion of the pro- and post-glacial sediments (Unit 4) where they onlap the bank tops indicates deeper water deposition due to isostatic depression. Withdrawal of the Hudson Strait ice margin terminated the supply of limestone and allowed the re-establishment of the modern current regime resulting in

deposition of the current moulded Holocene muds which are nearly devoid of limestone.

Geotechnical Sampling, Testing and Analysis

This study concentrates on the sampling, testing and analysis of cores from three cruises: six cores from Hudson HU84-035, five cores from HU83-030, and eight cores from HU82-054. The data from HU82-054 has been previously reported (Silva et al., 1983). The locations of all core stations appear in Table 2.

Subsampling of the HU84-035 cores was done on board ship and testing was completed at URI/MGL. Shipboard operations included removal of sections for consolidation testing, vane shear measurements and subsampling for bulk density, water content and Atterberg limits. Consolidation samples, approximately 6 cm long, oriented perpendicular to bedding, were cut from the full-round cores. These were subsequently subsampled by manually pushing a thin-walled 5.1 cm I.D. stainless steel ring into the sediment. Samples were trimmed from the subsection, capped with plexiglass plates, waxed, and refrigerated. They were then hand carried to URI where they were stored in sea water at 4° C until testing.

Similar techniques were employed to obtain the HU82-054 and HU83-030 samples. Four additional 3.6 cm I.D. consolidation samples, oriented parallel to bedding, were secured from split HU82-054 cores stored at BIO.

On HU84-035, vane shear measurements of peak undrained shear strength were taken approximately every 15-30 cm in the split cores, except PC15; which was disturbed and PC18 which was not split on board ship. A motorized

Wykeham Farrance vane shear device was utilized with a 12.7 x 12.7 mm vane, at a rotation rate of 60°/minute. Bulk density/water content samples were obtained with a constant volume sampler as near to the vane shear measurements as possible. All water contents are based on percent dry weight and corrected for 35 ppt salt. Specific gravity measurements were made using standard pycnometer flasks, according to ASTM Standard D854. Atterberg limits (ASTM Standards D423 and D424) were performed on bulk samples at approximately 30-50 cm intervals.

Grain size analyses on HU84-035 samples done at BIO used a Micromeritics Automatic Size Analyzer. Grain size measurements at URI/MGL were performed by the pipette method (Folk, 1974) after the fine fraction was separated by wet sieving through a 63 μ m screen.

Ancillary work included scanning electron microscopy (SEM) and energy dispersive X-ray spectrometry (EDS), lithologic determinations and calcium carbonate analyses on selected samples. SEM/EDS samples were freeze dried, and viewed in the instrument at magnifications of up to 12000 X.; the results were inconclusive however. Qualitative lithology determinations, completed at BIO on HU82-054, HU83-030 and HU84-035 samples, involved visual inspection of the > 63 μ m fraction with a petrographic microscope and testing with HCl. Lithologic components were identified as crystalline, clastic, metasedimentary and carbonate. In addition, quantitative determinations of percentage CaCO₃ were performed at URI using the carbonate bomb technique of Muller and Gastner (1971).

Consolidation tests were performed in standard oedometers in general accordance with ASTM Standard D2435. Load increment ratios (LIR) were

varied to facilitate both rapid testing and to best define the consolidation curve. A LIR of 0.5 was employed to define the break in the $e \log \sigma'$ curve, while a LIR of 1.0 was used to define the straight (virgin) portion of the graph. Preconsolidation stresses are determined by the Casagrande (1936) method. Overburden stresses are estimated from density profiles derived from the specific gravity and water content measurements. Overconsolidation ratios (OCR) are calculated as the ratio of preconsolidation stress to vertical effective overburden stress. OCR values greater than about 1.2 signify overconsolidation, whereas values below about 0.7 indicate underconsolidation. Values in the intermediate range of 0.7 to 1.2 indicate normal consolidation.

It should be emphasized that many surficial (0-3m) marine sediments exhibit varying degrees of "apparent overconsolidation" (AOC). This phenomenon is attributed to strong interparticle bonding which occurs in fine-grained marine sediments generating an inherent strength greater than the overburden pressure. It can complicate interpretation of consolidation test results, making it necessary to consider other properties such as shear strength, water content, Atterberg limits and texture in order to fully understand the stress history.

The compression index (C_c), a measure of the sample's compressibility, was calculated as the slope of the virgin curve portion of the $e \log \sigma'$ plot. The coefficient of consolidation (c_v) and the coefficient of permeability (k) were determined from consolidation test data using procedures developed by Casagrande (1936) and Taylor (1948).

Results of all consolidation tests were re-evaluated using the strain

energy technique, after Tavenas et al. (1979). The result is a linear plot of the sum of strain energy vs vertical effective stress. This method is purported to overcome the problems of apparent overconsolidation and cementation (K. Moran, personal comm.).

A comparison of preconsolidation stresses and OCR values as estimated by the conventional (Casagrande, 1936) and the strain energy (Tavenas et al., 1979) techniques may be found in Table C-1 in the Appendix. In addition, three plots are displayed in Figures C-1, C-2 and C-3. Figure C-1 is an example of an ideal graph. Two straight lines with different slopes intersect at a stress greater than zero, theorized to represent the value of preconsolidation stress (Tavenas et al., 1979). On the other hand, Figure C-2 is typical of a number of samples where the two portions of the graph intersect at a stress less than zero, obviously an impossible situation. Figure C-3 is representative of the third type of plot, wherein several intersections are visible. Several samples resulted in graphs where straight lines could not be drawn.

Inspection of Table C-1 reveals significant disagreement between the two methods, even in cases where the graphs were considered good for each technique. Based on these results, the strain energy method appears to generate less reasonable and less consistent results. It frequently seems to overestimate the preconsolidation stress and OCR and therefore has been judged to be not appropriate for this study of glacio-marine sediments.

Summary of Properties

Composite graphs of sedimentologic properties and seismic profiles

correlated to the sampling sites are presented in Figures 7 through 20. Tables of this data may be found in Table A-3 through A-5 and in the Appendix. Although tests were performed on HU84-035-015, the data is not presented because it was later determined that this core had fallen over or otherwise sucked in sediment on impact with the seafloor. Therefore this core does not represent a true stratigraphic section.

Core HU82-054-013 recovered sediment of Units 5b, 4 and 3b (Fig. 7). Both Units 5b and 4 contain lithic carbonate fragments and a number of foraminifera species. Unit 3b, on the other hand, is devoid of both forms of CaCO_3 . Water contents and shear strengths increase gradually downcore, to the top of Unit 3b, below which shear strengths increase dramatically and water contents decrease. Unit 5b has a high silt content and a small percentage of clay compared to Units 4 and 3b.

Core HU83-030-036 (Fig. 8) also recovered Units 5b, 4 and 3b, and exhibits properties similar to those of HU82-054-013. Water content ranges are similar, but decrease fairly uniformly throughout core HU83-030-036. Shear strengths appear more variable in HU83-030-036 than HU82-054-013, but exhibit the same increasing trend with depth, and a sharp increase at the top of Unit 3b. Again, no lithic or biogenic calcium carbonate was discovered in Unit 3b. However, significantly smaller percentages of CaCO_3 are present in Units 5b and 4.

Core HU82-054-015 retrieved samples of Units 4 and 3b (Fig. 9). The sediment tends to be fairly coarse-grained and when compared to other cores, displays a high degree of variability in the properties examined. Clay contents and water contents exhibit sharp increases at approximately 100 cm,

whereas shear strengths increase regularly to the bottom of Unit 4. A dramatic increase in shear strength occurs at the top of Unit 3b, to the highest recorded values for these cores. Lithic carbonate and foraminifera percentages resemble those of HU82-054-013 (Fig. 7).

HU84-035-016 was the only core which recovered Unit 3c, the Hudson Strait Till (Fig. 10). Its characteristics are similar to those of Unit 4, although it tends to be coarser-grained and contains more foraminifera. Water contents are nearly uniform with depth, while shear strengths display a gradual increase. Lithic carbonate contents are among the highest measured in this study.

Core HU84-035-014 which contains Unit 4 exclusively, exhibits variable properties and few real trends with depth (Fig. 11). Shear strength values increase dramatically at approximately 400 cm, but are not accompanied by any other significant property variations. The sediment becomes finer-grained with depth. The higher shear strength may be related to ice scouring and resulting overloading of deeper strata.

Unit 5b, sampled in HU82-054-004 (Fig. 12) is coarse-grained, with low water contents and fairly high shear strengths. In Unit 5a (HU82-054-014, Fig. 13), the lithic fraction is composed almost entirely of crystalline sediment. Shear strengths are relatively low, but increase gradually with depth. Water contents show a general decrease with depth.

Both HU84-035-008 and 011 (Figs. 14 and 15) were cored in the Davis Strait and contain silts which are the equivalent of Unit 4 (Davis Strait Silt of Praeg et al., 1986). Shear strengths tend to increase with depth in both cores, but are generally higher in HU84-035-011. Water contents are

nearly uniform in both cores but are considerably lower in core HU84-035-011 than in HU84-035-008.

HU82-054-002, 005 and 006 (Figs. 16, 17 and 18) all retrieved a surface veneer of 5b, underlain by Unit 4. Water content and shear strength profiles for all three cores are similar. Water contents in Unit 5b are low and shear strength (measured only in core HU82-054-005) is high. In Unit 4, the water contents tend to decrease gradually with depth and shear strengths remain relatively uniform, or increase slightly. Unit 5b is fairly coarse grained (HU82-054-05); and Unit 4 is composed of nearly equal percentages of clay and silt.

Core HU83-030-020 recovered a surficial veneer of 5b (Fig. 19), approximately three meters of 5a, and six meters of Unit 4. The properties display a fairly high degree of variability, but general trends of decreasing water content and increasing (but variable) shear strengths below Unit 5b can be discerned.

Core HU83-030-026 (Fig. 20) is composed entirely of Unit 5c, the shelf-edge silty gravel. No real trends with depth are apparent and properties exhibit considerable variability.

Analysis and Discussion

Geotechnical testing was done on samples of three sedimentary units on the Labrador Shelf. The lateral distribution of these units is shown in Figure 3. Unit 3a has not been adequately sampled because it is either too consolidated or too bouldery. Unit 3b is less laterally extensive than Unit 3a and its surface is iceberg scoured in most areas. Samples of this

subunit have been retrieved in HU82-054-013, 015, 016, and HU83-030-036 (see Figs. 7, 8, 9). Unit 3c, the Hudson Strait Till, has been derived from reworking of the glacial marine sediments of Unit 4 by a large grounded ice sheet. It overlies and is interfingered with Unit 4. It is believed that Unit 3c was recovered in core HU84-035-016 (Fig. 10).

Unit 4 is a well stratified, conformable deposit with abundant carbonate fragments. Ice rafted clasts are common and typically the unit fines upward. All cores except HU82-054-014, HU83-030-026 and HU84-035-018 retrieved Unit 4.

Unit 5, a modern, post-glacial deposit, is also divided into subunits. Unit 5a is a finely stratified mud and nearly transparent acoustically. Restricted to deep regions of the shelf, it was recovered in HU82-054-014 (Fig. 13) and HU84-035-018. Carbonate fragments are rare or absent. Unit 5b (Fig. 12) is weakly stratified acoustically and occurs on bank tops. It results largely from winnowing of the underlying till. Unit 5b was identified as a surface veneer, less than one meter thick, in several cores. At the shelf edge, Subunit 5c (Fig. 20) onlaps the continental shelf. This unit is highly variable laterally and cannot be adequately represented by one core (HU83-030-026).

The upper till, Unit 3b, exhibits different characteristics dependant upon the region of deposition. Two cores (HU82-054-013 and 015) near the pinch out of the unit believed to be the edge of the ice sheet display significant overconsolidation, relatively high shear strengths and low water contents (Table 5). Piston core HU83-030-036, on the other hand, taken in deeper water within the saddle, is normally consolidated (Table 5).

Furthermore, at comparable depths within the cores, the shear strengths are considerably lower in HU83-030-036 (see Figures 7, 8 and 9). The hypothesis advanced is that the ice was essentially hydrostatically supported in the deeper regions, whereas grounding of the ice sheet near the periphery resulted in basal loading of the underlying deposits.

The Hudson Strait Till (Unit 3c) is similar to Unit 4 (lithologically and texturally to some degree) because it is derived from reworking of the latter deposit. Water contents in Unit 3c (core HU84-035-16) are generally higher and shear strengths much lower than those in Unit 3b or Unit 4 (Fig. 10). Based on the low shear strengths, relatively high water contents, and the extreme water depth (over 600m), we conclude that the Unit 3c material at this location and water depth did not experience appreciable ice loading (Table 5). Subbottom acoustic data appears to verify this by indicating that iceberg scouring has not occurred here.

Because of the large number of samples recovered from Unit 4, it is the most completely described. Peak undrained shear strengths range between approximately 4 and 16 kPa. Water contents of 18-68% have been measured. Typical values of Atterberg limits are 17% for plastic limit and 32% for liquid limit. In situ water contents are generally greater than the liquid limit. Overconsolidation ratios vary widely but Unit 4 is primarily normally consolidated. Some exceptions are discussed below.

Water content and shear strength profiles of cores HU84-035-008 and 011 show that the scouring process decreases water content and increases the shear strength by consolidating the sediment. However, these observations must be tempered with due consideration for textural differences which can

greatly influence these properties. Both cores recovered sediment of the Unit 4 type and are only 23 km apart. The difference between the two cores is that HU84-035-008 is unscoured (see seismic section in Fig. 14), whereas HU84-035-011 is in a region which has been extensively scoured (Fig. 15). In HU84-035-011 the shear strength values are about double and the water contents are approximately half of those in HU84-035-008, but the consolidation test results suggest that iceberg loading at site HU84-035-011 was minimal (Table 5). Nevertheless, based on available data, the action of iceberg scouring is theorized to be the primary cause of the differences in properties.

Additional evidence to support the theory that iceberg scouring increases shear strength and consolidates the deposit is a consistent, albeit highly qualitative correlation between depth of core penetration and the degree of iceberg scouring. Piston cores recover significantly shorter samples in scoured deposits than in unscoured regions, and gravity cores have failed to retrieve any material in scoured sediment.

One consideration which has not been adequately analysed as yet is the rate of consolidation as related to the loading time associated with iceberg scouring. Even if the loading is very high, it takes appreciable time for fine-grained sediments to dewater and the analysis should account for both lateral and vertical drainage conditions. The consensus of opinion is that a drainage boundary at the ice-sediment interface would have been operative, due to the saline environment, and that lateral drainage would contribute to consolidation during the time of iceberg grounding. Therefore, it is assumed that any significant overloading due to iceberg grounding would be

reflected in consolidation stress history of recovered samples. This aspect of the problem warrants additional analyses beyond the scope of the current studies.

Unit 4 at sites HU82-054-004, 005 and 006 exhibits very similar properties and characteristics. The shear strengths are low, and water contents are relatively high. The moderately high overconsolidation ratios of the shallow samples are attributed to apparent overconsolidation rather than effects of overburden loading (Table 5). We conclude that Unit 4, sampled in central Karlsefni Trough has not experienced significant loading from ice processes. Along the flanks of the trough, where iceberg scouring is much more common, no piston core penetration was successful, suggesting consolidation of the sediment by scouring or excess loading.

Some anomalous situations exist in Unit 4. Core HU84-035-016, for instance, contains a normal to underconsolidated sample at 365 cm and a significantly overconsolidated sample at 473 cm (Table 5). Both samples were of very good quality and displayed similar permeabilities and compression indexes. The possibility of scouring followed by continued deposition is supported by higher shear strength and slightly lower water content in the deeper sample compared to those in the sample at 365 cm. A similar scenario may be envisioned in core HU84-035-014, also in Hudson Strait, based on like reasoning. Here, overconsolidation ratios greater than unity below 3.0 m suggest some iceberg loading prior to deposition of the shallower sediment.

Only one core from Unit 5c was tested in this program (HU83-030-026). The data suggest a highly variable unit. The single consolidation test

yielded an OCR of 2.3 which is attributed to apparent overconsolidation (Table 5). All the stratigraphic and physical property evidence indicates that these sediments have not been significantly affected by ice loading or scouring.

Unit 5b was recovered as a surface veneer (less than one meter thick) in several cores. This material was not sampled extensively and only a few general observations can be made. Texturally, it is fairly coarse. Water contents are low and shear strengths and bulk densities are high, relative to those in Units 4 and 5a (see Figs. 8, 9, 13, 17, 18 and 20).

Conclusions:

In conclusion, we make the following summary observations:

- Unit 3b, the Upper Till, is overconsolidated in shallow water near the ice sheet perimeter, due to the action of ice grounding and/or scouring.
- In deep water, the sediments of Unit 3b are normally consolidated and have not experienced any significant loading.
- Unit 3c, the Hudson Strait Till, where deposited in deep water is normally consolidated. We conclude that no appreciable ice loading has occurred.
- Unit 4 appears to be primarily normally consolidated with no evidence of ice loading except in two cores recovered in the northern region of the shelf. We hypothesize that in some parts of these northern areas iceberg scouring caused excess loading of the deeper strata which was subsequently followed by deposition of normally consolidated, non-scoured sediments.

- Based on evidence from this study, it appears that Unit 5c, at the shelf edge, is normally consolidated and has not experienced any ice loading.

Acknowledgements

We thank John Zevenhuizen and Linda Kiely (B.I.O.) for their efficient and careful data compilation. The following people from the University of Rhode Island were also involved in the program: S. A. Jordan. W. P. Levy and G. Chiarello on analysis and reporting of HU-82-054 and HU-83-030 results, and E. Cianciaruli on cruise HU-83-030. K. Moran was also very helpful in various aspects of the program. We thank Brian Maclean for providing the data from the Southern Baffin Shelf.

Reference List

1. Casagrande, A., 1936. The determination of the pre-consolidation load and its practical significance. Proc. Int'l. Conf. Soil Mech., Vol. III, Harvard Univ. Cambridge, p. 60.
2. Dadey, K., 1984. Cruise Report, HUDSON 84-035 Cruise, University of Rhode Island (unpublished)
3. Folk, R. L., 1974. Petrology of Sedimentary Rocks. Hemphills, Austin, 135 pp.
4. Josenhans, H., Zevenhuizen, J. and Klassen, R. A., 1986. The Quaternary geology of the Labrador shelf, Canadian Journal Earth Science (in press).
5. Müller, G. and Gastner, M., 1971. The "Karbonat and Bombe," a simple device for determination of carbonate content in sediments, soils and other materials. Neves Jahrb. Mineral Monatsh, 10:466-469.
6. Praeg, D. B., MacLean, B., Hardy, I. A., and Mudie, P. J., in press. Quaternary eology of the southeast Baffin Island continental shelf, N.W.T., Geological Survey of Canada, Paper 85-14.
7. Silva, A. J., Levy, W. P., Jordan, S. A. and Cianciaruli, E., 1984. Geotechnical properties of Labrador shelf sediments: HUDSON 83-030 cruise (draft) University of Rhode Island.
8. Silva, A. J., Josenhans, H. W., Jordan, S. A., Levy, W. P., 1983. Geotechnical Analysis of Labrador Shelf Sediments: HUDSON-82-054 Cruise for Petro Canada, Project Report No. PC83-1.
9. Tavenas, F., Desrosiers, J. P., Leroueil, S., LaRochelle, P. and Roy,

H., 1979. The use of strain energy as a yield and creep criteria for lightly overconsolidated clays. *Geotechnique*, 29:285-303.

10. Taylor, D. W., 1948. Fundamentals of Soil Mechanics. John Wiley & Sons, NY, 700 pp.

Figure Captions

- Fig. 1. Location map showing position of seismic sections (after Josenhans et al., 1986).
- Fig. 2. Acoustic stratigraphy contour map (after Josenhans et al., 1986).
- Fig. 3. Lateral distribution of acoustic/stratigraphic units (after Josenhans et al., 1986).
- Fig. 4. Location map showing position of cores (after Josenhans et al., 1986).
- Fig. 5. Idealized section through Nain Bank and Outer Hopedale Saddle (after Josenhans et al., 1986).
- Fig. 6. Seismic section through Hopedale Saddle (x-y in Fig. 1; after Josenhans et al., 1986).
- Fig. 7. Summary of properties and associated seismic section: HU82-054-013 (adapted from Josenhans et al., 1986).
- Fig. 8. Summary of properties and associated seismic section: HU82-030-036 (adapted from Josenhans et al., 1986).
- Fig. 9. Summary of properties and associated seismic section: HU82-054-015 (adapted from Josenhans et al., 1986).
- Fig. 10a. Summary of properties HU84-035-016 (adapted from Josenhans et al., 1986).
- Fig. 10b. Seismic section associated with Fig. 10a (HU84-035-016).
- Fig. 11. Summary of properties and associated seismic section: HU84-035-014 (adapted from Josenhans et al., 1986).
- Fig. 12. Summary of properties and associated seismic section: HU82-054-004 (adapted from Josenhans et al., 1986).
- Fig. 13. Summary of properties and associated seismic section: HU82-054-014 (adapted from Josenhans et al., 1986).

Fig. 14a. Summary of properties HU84-035-008.

Fig. 14b. Seismic section associated with Fig. 14a (HU84-035-008).

Fig. 15a. Summary of properties HU84-035-011.

Fig. 15b. Seismic section associated with Fig. 15a (HU84-035-011).

Fig. 16. Summary of properties: HU82-054-002 (from Silva et al., 1983).

Fig. 17. Summary of properties: HU82-054-005 (from Silva et al., 1983).

Fig. 18. Summary of properties: HU82-054-006 (from Silva et al., 1983).

Fig. 19. Summary of properties: HU83-030-020 (from Silva et al., 1983).

Fig. 20. Summary of properties: HU83-030-026 (from Silva et al., 1983).

C-1 Sum of strain energy vs vertical effective stress: HU82-054-015 238 cm.

C-2 Sum of strain energy vs vertical effective stress: HU82-054-015 177 cm.

C-3 Sum of strain energy vs vertical effective stress: HU82-054-006 126 cm.

Table 1: Lithology and Stratigraphic Relationships
Of Geological Units at or near the
Seabed on the Labrador Shelf

<u>Period</u>	<u>Epoch</u>	<u>Unit</u>	<u>Lithology</u>
Quaternary	Recent	(5) Post-glacial marine sediments	5a. stratified sediment consisting mostly of clay and silt with minor sand and gravel; 5b. reworked sediments consisting mostly of sand with minor silt and gravel (locally gravel predominates over sand) 5c stratified sediments, texturally highly variable (confined to shelf edge)
	Pleistocene	(3) & (4) Glacial and glaciomarine deposits	4. pro- and post glacial sediments. Conformable to unconformable contact 3. glacial till (3c. Hudson Strait Till, 3b. Upper Till, 3a. Lower Tills) Unconformable contact
	Pliocene	(2) Tertiary Bedrock	2a. Saglek Formation, feldspathic and cherty conglomeratic sandstone with minor siltstone and claystone
Tertiary	Miocene		Unconformable 2b. Mokami Contact Formation. Claystone and shale with minor siltstone, sandstone and limestone
	Oligocene		Unconformable contact
Precambrian		(1) Acoustic Basement	Granite and metamorphic rocks of the Nain, Churchill and Grenville provinces.

Table 2: Summary of Coring Results

Core	Sed. Recovered (cm)	Position		Condition
		Latitude	Longitude	
<u>HU84-035</u>				
Frobisher Bay Mouth				
PC008	820	61°47.2'N	63°49.9'W	Gassy
PC011	380	61°54.5'N	62°28.0'W	Good
Hudson Strait				
PC014	530	60°59.2'N	62°27.3'W	Good
PC015	760	60°59.9'N	62°53.6'W	Poor
PC016	520	60°59.8'N	63°11.4'W	Good
Hopedale Saddle				
PC018	1110	55°53.9'N	58°40.4'W	Gassy
<u>HU83-030</u>				
Karlsefni Trough				
GC014	177	58°50.3'N	61°43.0'W	Good
S. Saglek Okak Bank				
PC020	836	58°17.0'N	61°43.7'W	Good
GC026	284	58°11.2'N	59°47.2'W	Good
Nain Bank Hopedale Saddle				
PC035	621	56°8.0'N	58°37.4'W	Poor
PC036	488	56°4.1'N	58°54.8'W	Good
<u>HU82-054</u>				
Karlsefni Trough				
PC002	464	59°16.6'N	63°04.1'W	Good
GC004	160	58°52.9'N	61°46.5'W	Good
GC005	266	58°52.9'N	61°46.6'W	Good
GC006	246	58°52.9'N	61°47.3'W	Good
Hopedale Saddle				
PC013	264	56°26.4'N	59°38.4'W	Good
PC014	1086	56°26.1'N	59°53.2'W	Good
Cartwright Saddle				
PC015	335	54°52.4'N	55°44.7'W	Good
PC016	378	54°51.8'N	55°27.4'W	Poor

Table 3: Summary of Geotechnical Testing Program
Labrador Shelf Sediments

Station	Water Content Tests	Measured Wet Bulk Densities	Specific Gravity Tests	Atterberg Limit Tests	Grain Size Tests*	Vane Shear Tests	Consol. Tests
Karlsefni Trough		a) <u>HU 82-054 Cruise</u>					
2	22	6	3	2	(2)5	21	1
4	10	9	3	1	(3)3	9	1
5	17	14	2	1	(2)2	14	1
6	13	13	2	2	(2)2	11	2
Hopedale Saddle							
13	15	3	4	1	(3)5	8	1
14	52	17	4	4	(4)6	37	0
Cartwright Saddle							
15	19	0	7	4	(5)8	16	2
16	18	1	2	2	(2)6	15	0
South Saglek - Okak Bank		b) <u>HU-83-030 Cruise</u>					
20	37	25	4	4	(4)8	35	4
26	11	11	2	2	(2)	11	1
Main Bank - Hopedale Saddle							
36	23	19	5	5	(5)14	23	3
Frobisher Bay Mouth		c) <u>HU-84-035 Cruise</u>					
8	27	16	1	18	0	21	2
11	20	9	1	10	0	16	3
Hudson Strait							
14	25	10	1	13	6	23	5
16	32	4	1	12	5	30	3

* Value in parentheses represents number of pipette tests; other value is the number of analyses.

Table 4a: Consolidation Results of Labrador Shelf Sediments
Hudson 82-054 Cruise

Sta. No.	Depth (cm)	Water Cont. w_1 (%)	Specific Gravity G_s	Init. Void Ratio e_o	Comp. Index C_o	Comp. Ratio $C_o/1+e_o$	Precon. Stress σ'_o (kPa)	Overbur. Stress σ'_o (kPa)	Overcon. Ratio OCR	Unit	Sample Quality
002	310	35.9	2.76	1.03	0.27	0.13	34.3	25.4	1.4	4	VG
004	142	44.4	2.64	1.17	0.33	0.15	24.5	10.9	2.3	4	G
005	142	49.3	2.71	1.35	0.44	0.19	22.6	10.8	2.1	4	G/VG
006	126	41.0	2.82	1.21	0.44	0.20	21.6	10.1	2.1	4	VG
013	248	20.8	2.56	0.57	0.21	0.13	65.7	23.4	2.8	3b	VG
015	177	54.1	2.73	1.48	0.43	0.17	-	13.2	-	4	NG
015	238	18.7	2.70	0.51	0.20	0.13	66.7	19.3	3.4	3b	G/VG

Table 4b: Consolidation Results of Labrador Shelf Sediments
HUDSON 83-030 Cruise

Station No.	Depth cm	Water Content w_1 (%)	Specific Gravity G_s	Init. Void Ratio e_o	Comp. Index C_o	Comp. Ratio $C_o/1+e_o$	Precon. Stress σ'_o (kPa)	Overurden Stress σ'_o (kPa)	Overconsol. Ratio OCR	Unit	Sample Quality
020	218	65.5	2.78	1.93	0.52	0.18	-	11.2	-	4	NG
020	392	51.7	2.83	1.55	0.38	0.15	22	21.2	1.0	4	Poor
020	642	43.1	2.81	1.32	0.34	0.15	30	35.5	0.8	4	VG
020	776	46.4	2.79	1.36	0.37	0.16	38	43.2	0.9	4	VG
026	147	36.8	2.78	1.23	0.36	0.16	20	8.8	2.3	5c	VG
036	180	28.2	2.79	0.81	0.22	0.12	30	11.8	2.5	4	G
036	308	56.8	2.81	1.53	0.52	0.20	20	18.0	1.0	3b	VG
036	324	31.4	2.76	0.92	0.20	0.10	18	21.9	0.8	3b	VG
036	484	26.3	2.75	0.83	0.19	0.10	35	33.2	1.0	3b	VG

Table 4c: Consolidation Results of Labrador Shelf
Sediments HUDSON 84-035

Station No.	Depth (cm)	Water Content $w_1\%$	Specific Gravity G_s	Init. Void Ratio e_o	Comp. Index C_o	Comp. Ratio $C_o / (1 + e_o)$	Precon. Stress σ'_o (kPa)	Overburden Stress σ'_o (kPa)	Overcon. Ratio OCR	Unit	Sample Quality
008	87	52.9	2.78	1.47	.53	.21	28	5.7	4.9	4 equiv.	Fair
008	152	40.1	2.78	1.11	.31	.15	15	11	1.4	4 equiv.	G
011	87	25.5	2.78	0.71	.17	.10	21	14.6	1.4	4 equiv.	Fair
011	203	20.3	2.78	0.56	.14	.09	40	22	1.8	4 equiv.	VG
011	302	21.6	2.78	0.6	.15	.09	34	33.4	1.0	4 equiv.	VG
014	152	47.2	2.68	1.26	-	-	-	112	-	4	NG
014	209	41.8	2.68	1.12	.29	.14	16	15.7	1.0	4	G
014	302	32.1	2.68	0.86	.23	.12	-	23.9	-	4	NG
014	378	52.3	2.68	1.4	.44/.79	.18/.33	45	24.3	1.8		Fair
014	453	48.0	2.68	1.3	.4	.21	39	35.3	1.1	4	VG
016	152	41.3	2.80	1.15	.34/.15	.16/.07	-	13.2	-	3c	NG
016	365	36.9	2.80	1.03	.25	.12	18	33.8	0.5	4	VG
016	473	33.0	2.80	0.93	.26	.13	80	44.9	1.8	4	VG
018	186	74.8	2.65	1.98	.60	.20	32	16.5	1.9	5a	G

Table 5: Summary of Properties by Unit

Unit	Core	Location	* Water	Iceload**		+		Quality	w _i %	Interpre- tation
			Depth (m)	Berg	Sheet	Su(kPa)	OCR/z			
3b	82-13	H.S.	215	Y	Y	18/H	2.3/248	VG	21	OC
	83-36	H.S.	420	Y?	Y?	21/H	1.0/308	VG	57	NC
						20/H	0.8/324	VG	31	NC
						20/H	1.0/484	VG	26	NC
						22/H	3.4/238	G/VC	19	OC
82-15	C.S.	270	Y	Y	22/H	3.4/238	G/VC	19	OC	
3c	84-16	Hud.S.	603	N	Y	<5/N	-/-	NG	41	NC
4	82-2	Sag.B.	170	N	N	5/N	1.4/310	VG	36	?
	82-4	Kar.T.	170	?	N	3/N	2.3/142	G	44	AOC?
	82-5	Kar.T.	170	?	N	4/N	2.1/142	G/VG	49	AOC
	82-6	Kar.T.	170	?	N	4/N	2.1/121	VG	41	AOC
	83-20	S.Sag.B.	278	N	N	3/N	-/218	NG	66	NC
						10/N	1.0/392	P	52	NC
						10/N	0.8/642	VG	43	NC
						9/N	0.9/776	VG	46	NC
						11/N	2.5/180	G	28	AOC/OC
						6/N	-/177	NG	54	
						7/N	4.9/87	F	53	AOC
	84-8	Baf.S.		N	N	5/N	1.4/152	G	40	AOC
						10/N	1.4/87	F	26	AOC/OC
						16/N	1.8/203	VG	20	AOC/OC
						16/N	1.0/302	VG	22	NC
						3/L-N	-/152	NG	47	NC
	84-14	Hud.S.	603	Y	N	5/N	1.0/209	G	42	NC
						6/N	-/302	NG	32	NC
						7/N	1.8/378	VG	52	NC
						7/N	1.1/453	VG	48	NC
						7/N	0.5/365	VG	48	NC/UC
						9/N	1.8/473	VG	33	OC
	5a	82-14	H.S.	377	N	N	10/N			70
84-18		H.S.	500	N	N		1.9/186	VG	74	AOC
5c	83-26	Shelf.E.	400	N	N	9/N	2.3/147	VG	37	AOC

* H.S.: Hopedale Saddle
 C.S.: Cartwright Saddle
 Hud.S.: Hudson Strait
 Sag.B.: Saglek Bank
 OC = Overconsolidated
 NC = Normally consolidated
 AOC = Apparently overconsolidated

* Notation: Y = Yes, N = No

+ Notation: H = High, L = Low, N = Normal; (compared to average for core)

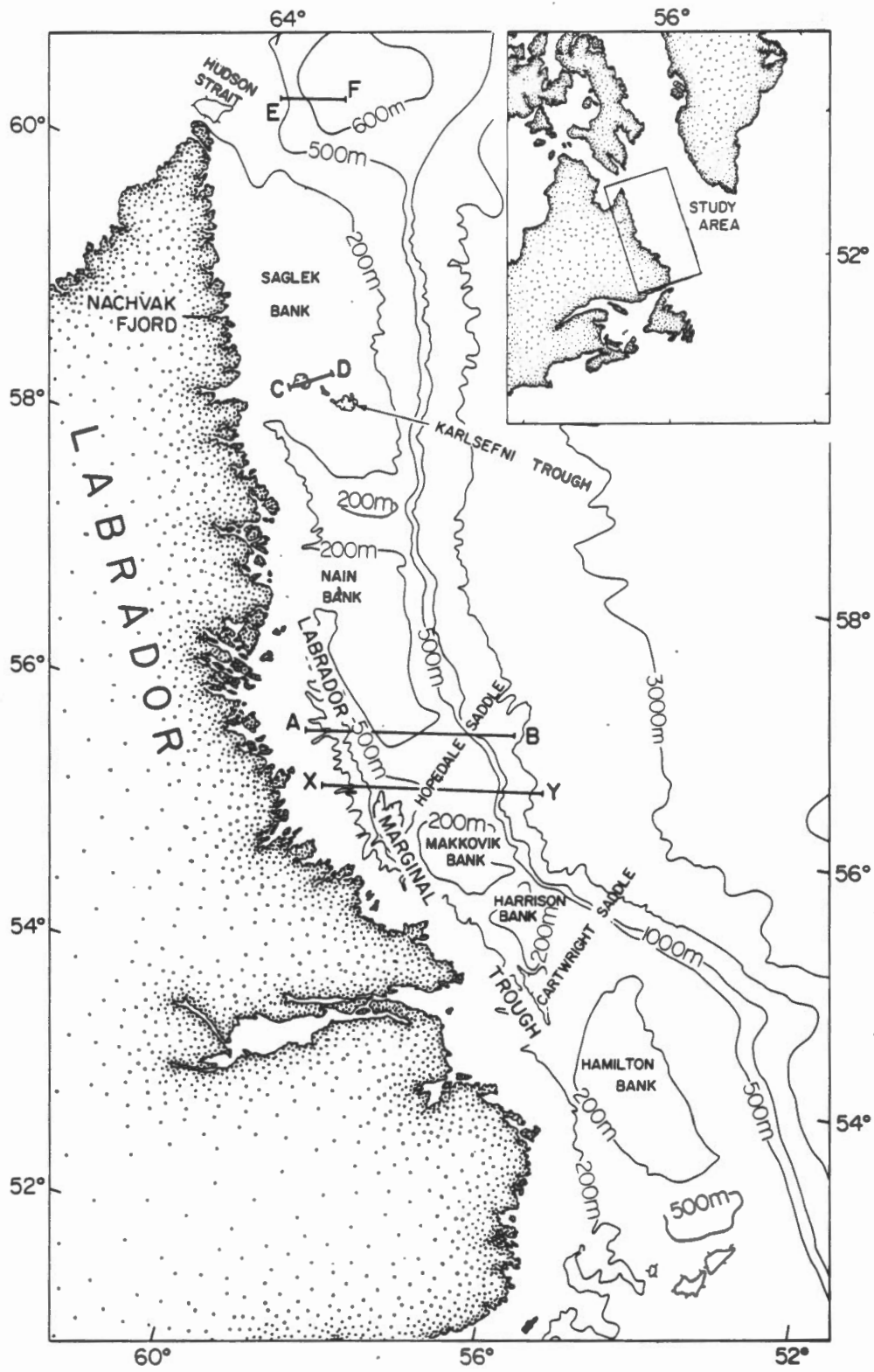


Fig. 1. Location map showing position of seismic sections (after Josenhans et al., 1986).

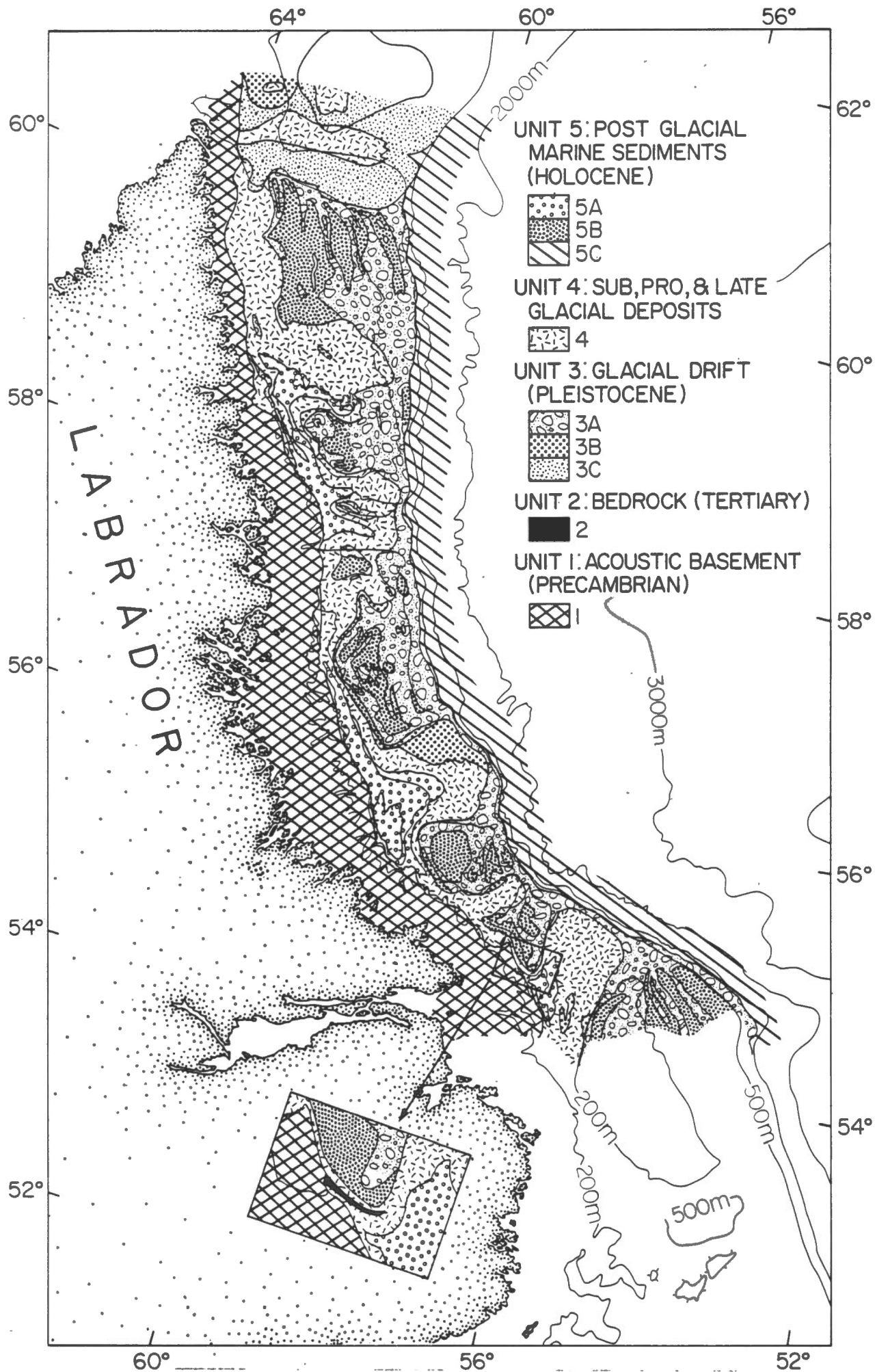


Fig. 3. Lateral distribution of acoustic/stratigraphic units (after

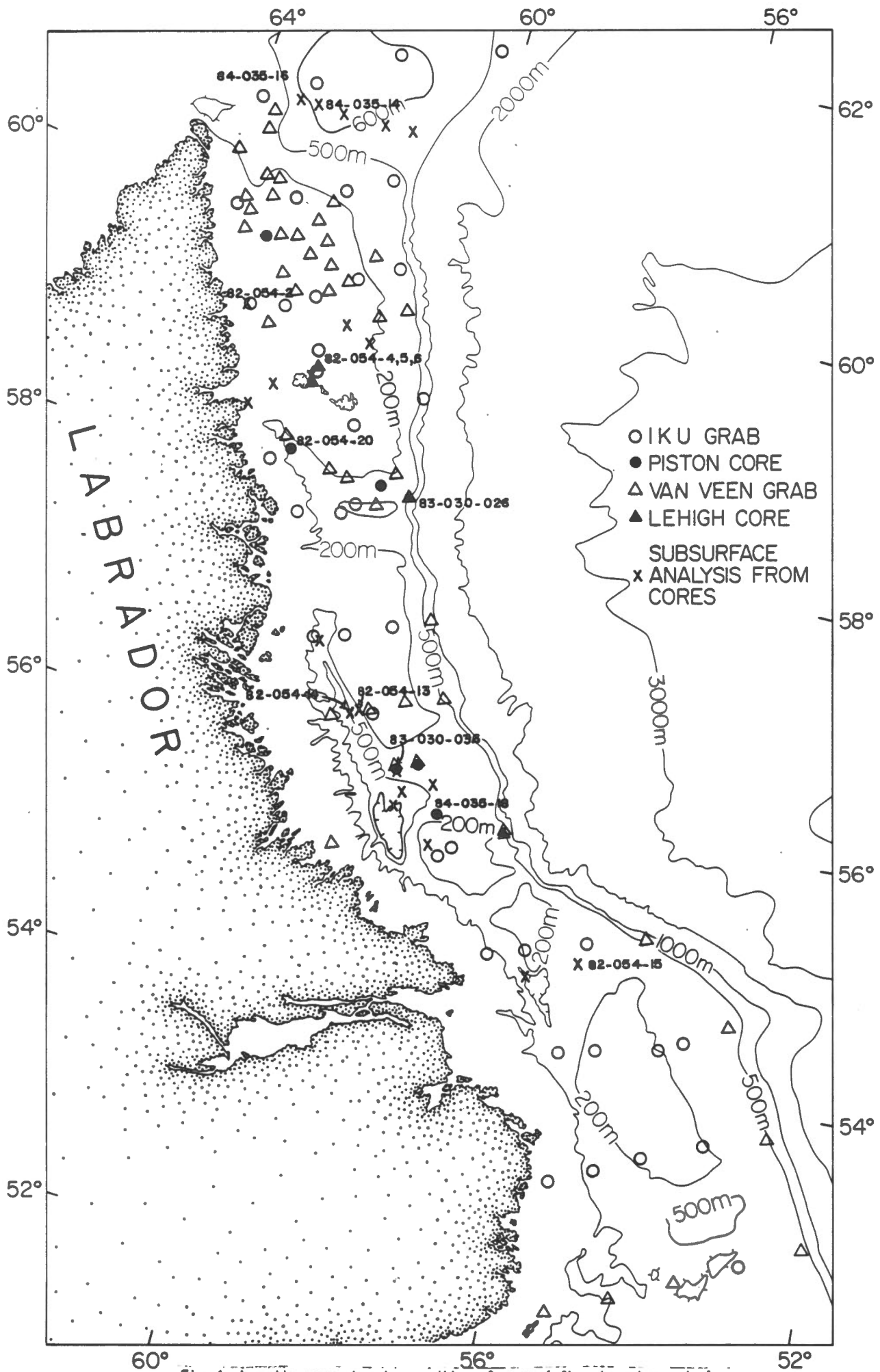


Fig. 4. Location map showing position of cores (after Josenhans et al.,

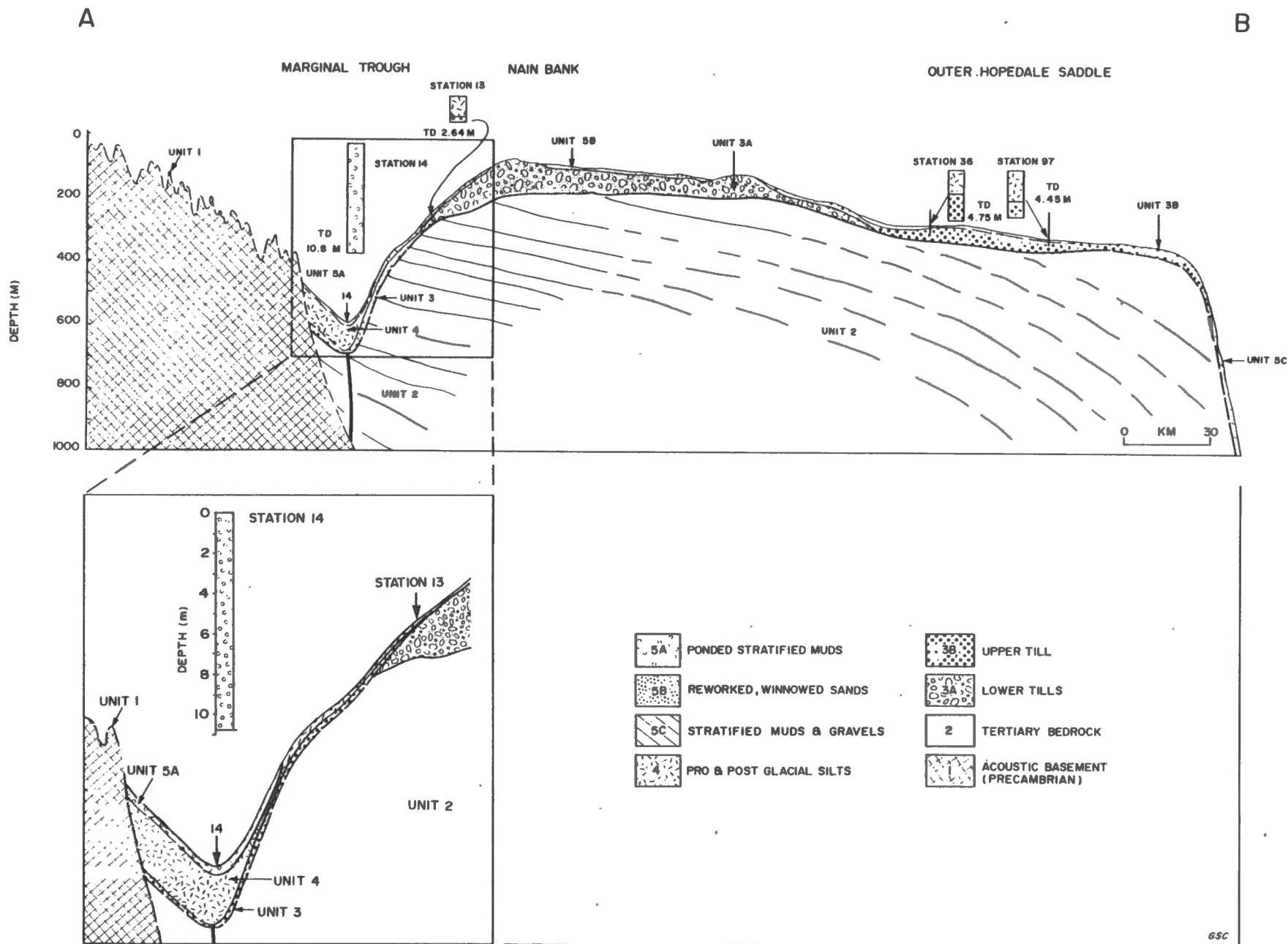


Fig. 5. Idealized section through Nain Bank and Outer Hopedale Saddle

(after Josenhans et al., 1986).

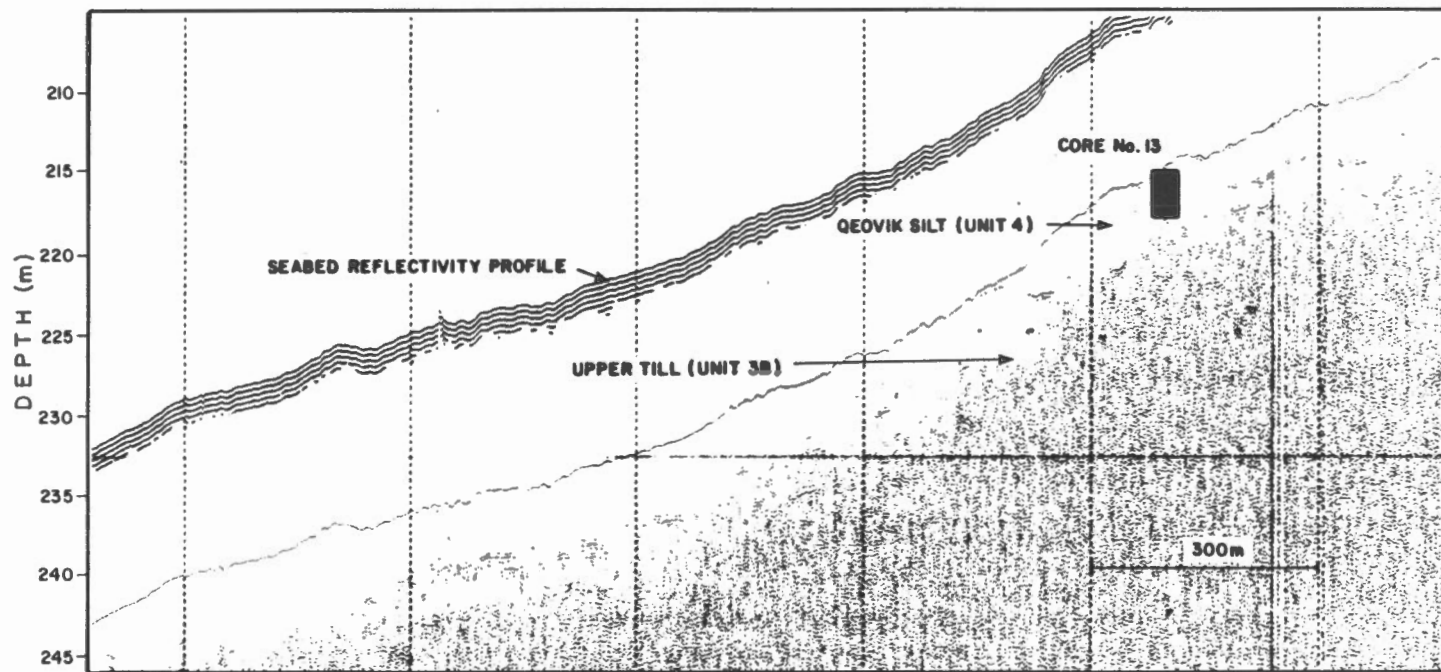
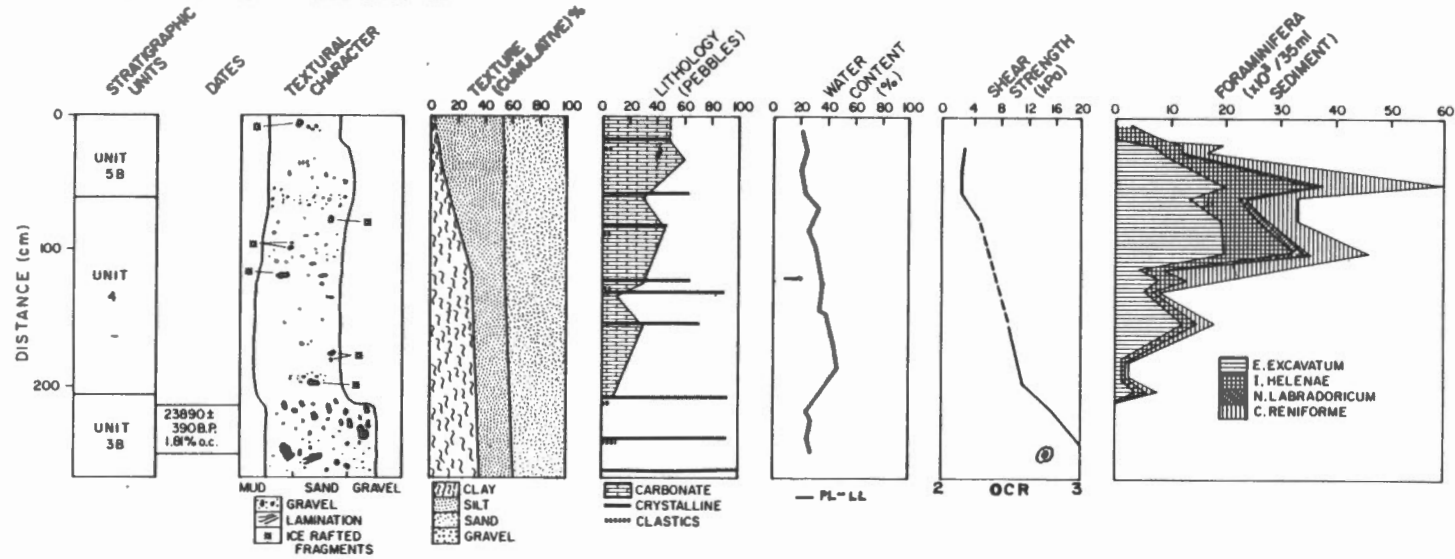


Fig. 7. Summary of properties and associated seismic section: HU82-

054-013 (adapted from Josenhans et al., 1986).

83-030-36 SEABED SLOPE 1:110 WATER DEPTH 420m

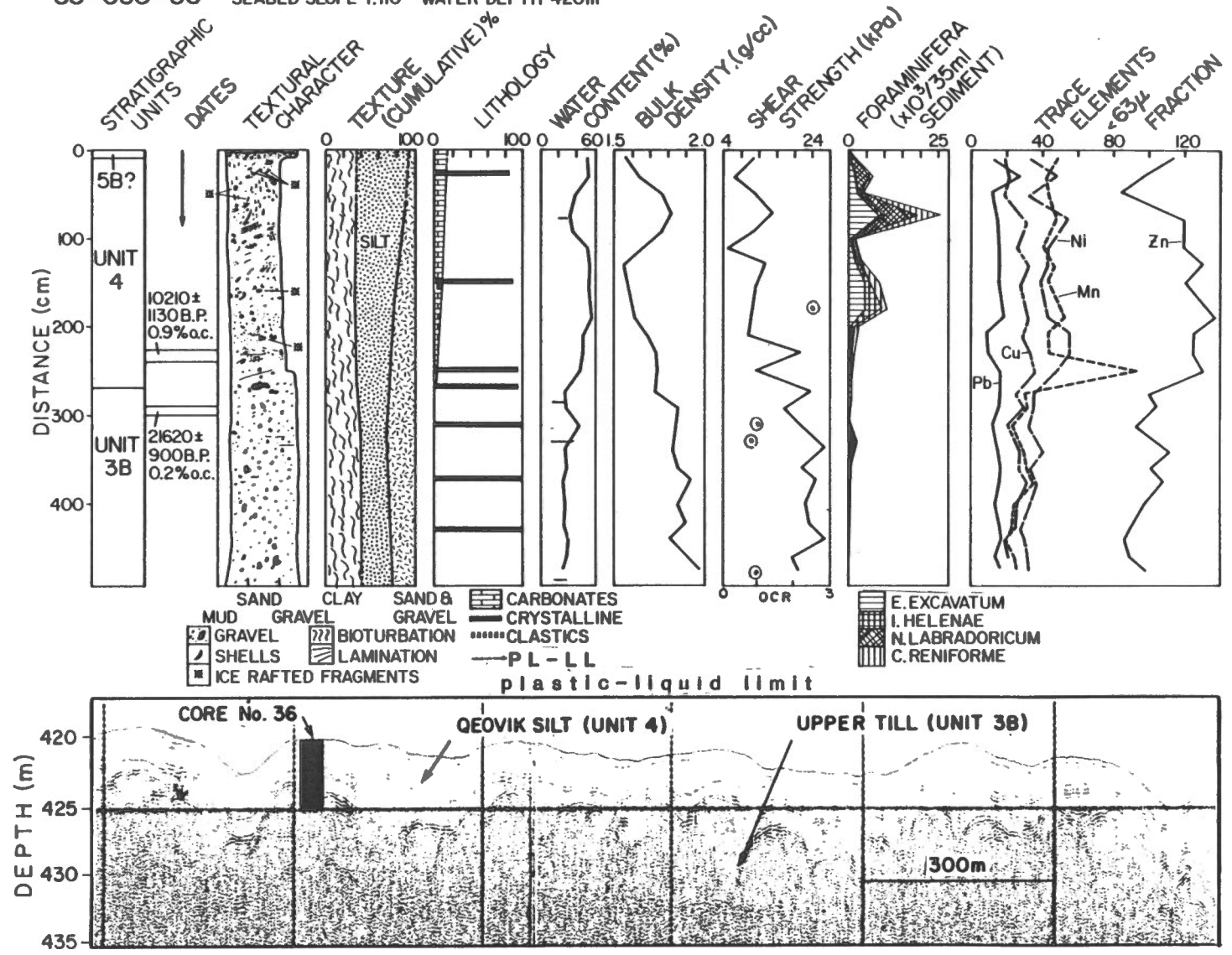


Fig. 8. Summary of properties and associated seismic section: HU82-

030-036 (adapted from Josenhans et al., 1986).

82-054-15 SEABED SLOPE 1:1068 WATER DEPTH 270m

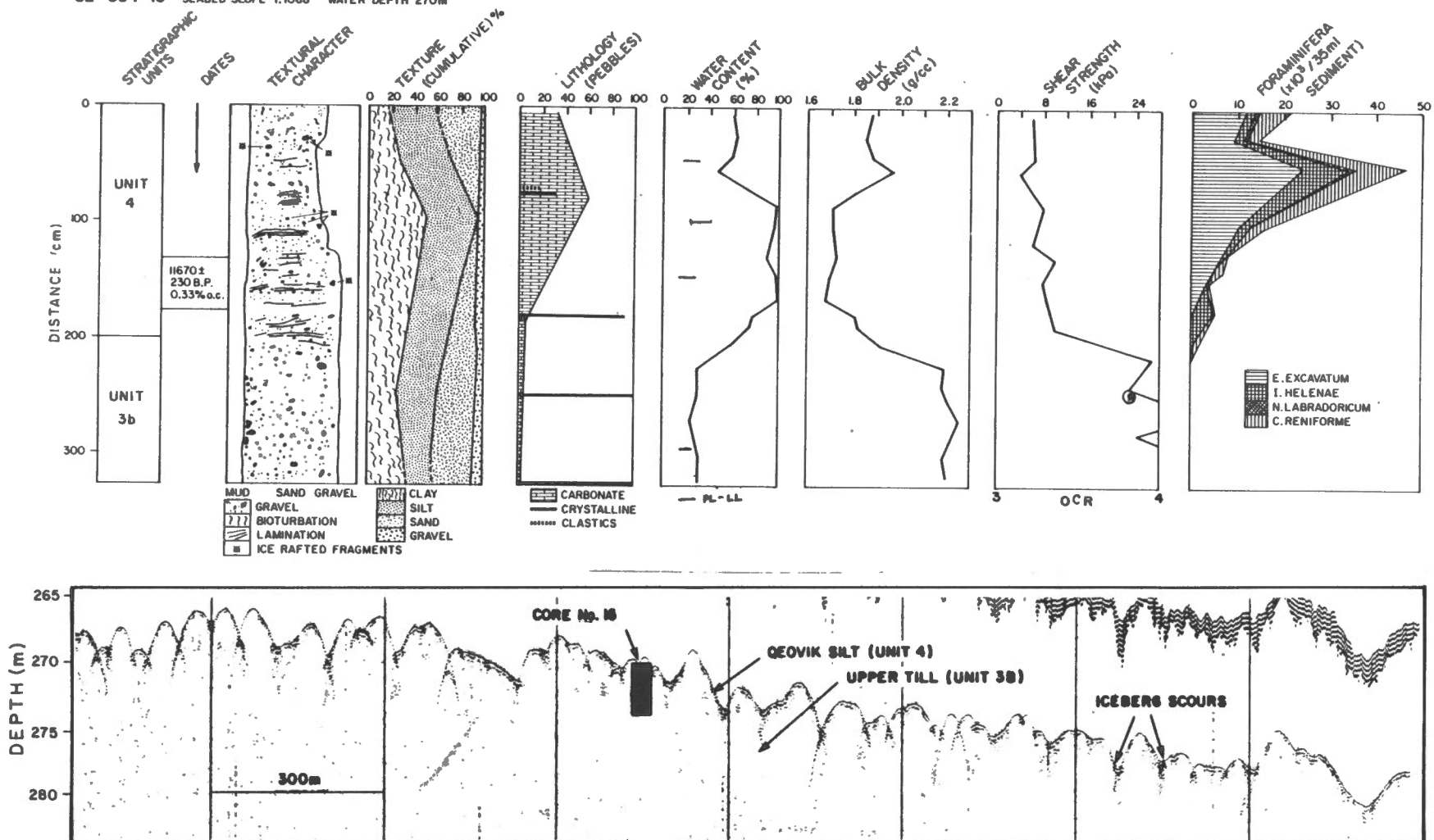


Fig. 9. Summary of properties and associated seismic section: HU82-054-015 (adapted from Josenhans et al., 1986).

84-035-16
Water Depth:
603M

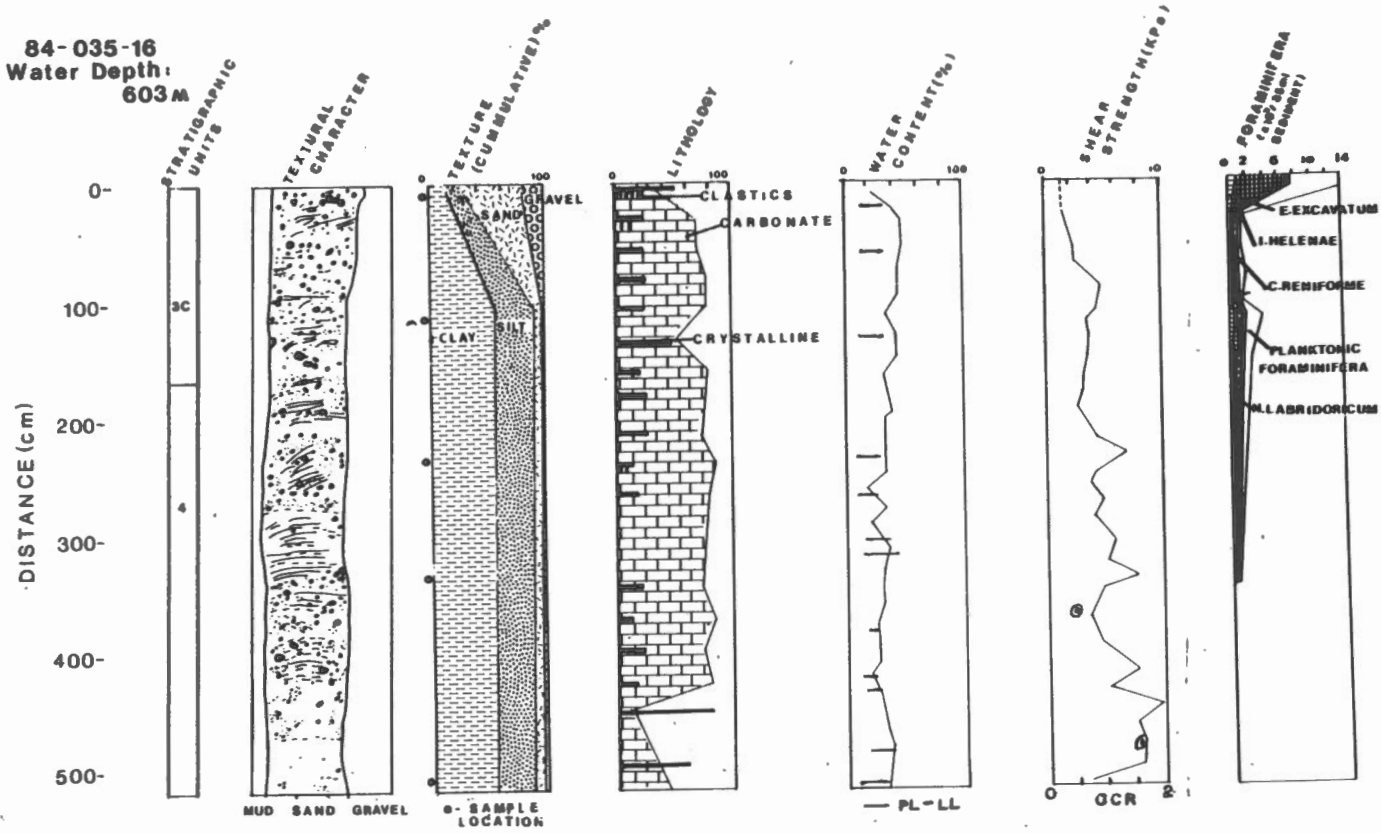


Fig. 10a. Summary of properties HU84-035-016 (adapted from

Josenhans et al., 1986).

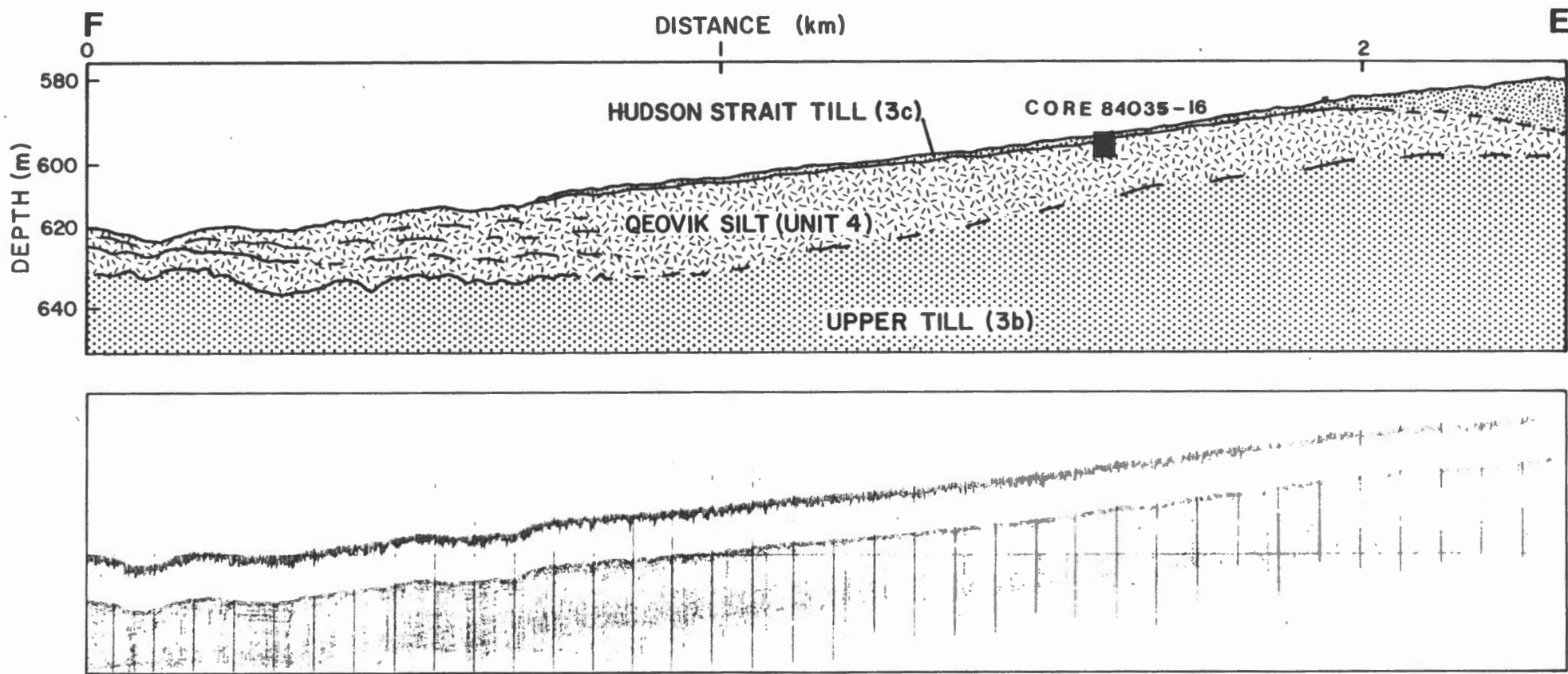


Fig. 10b. Seismic section associated with Fig. 10a (HU84-035-016).

84-035-14
 WATER DEPTH: 605 M

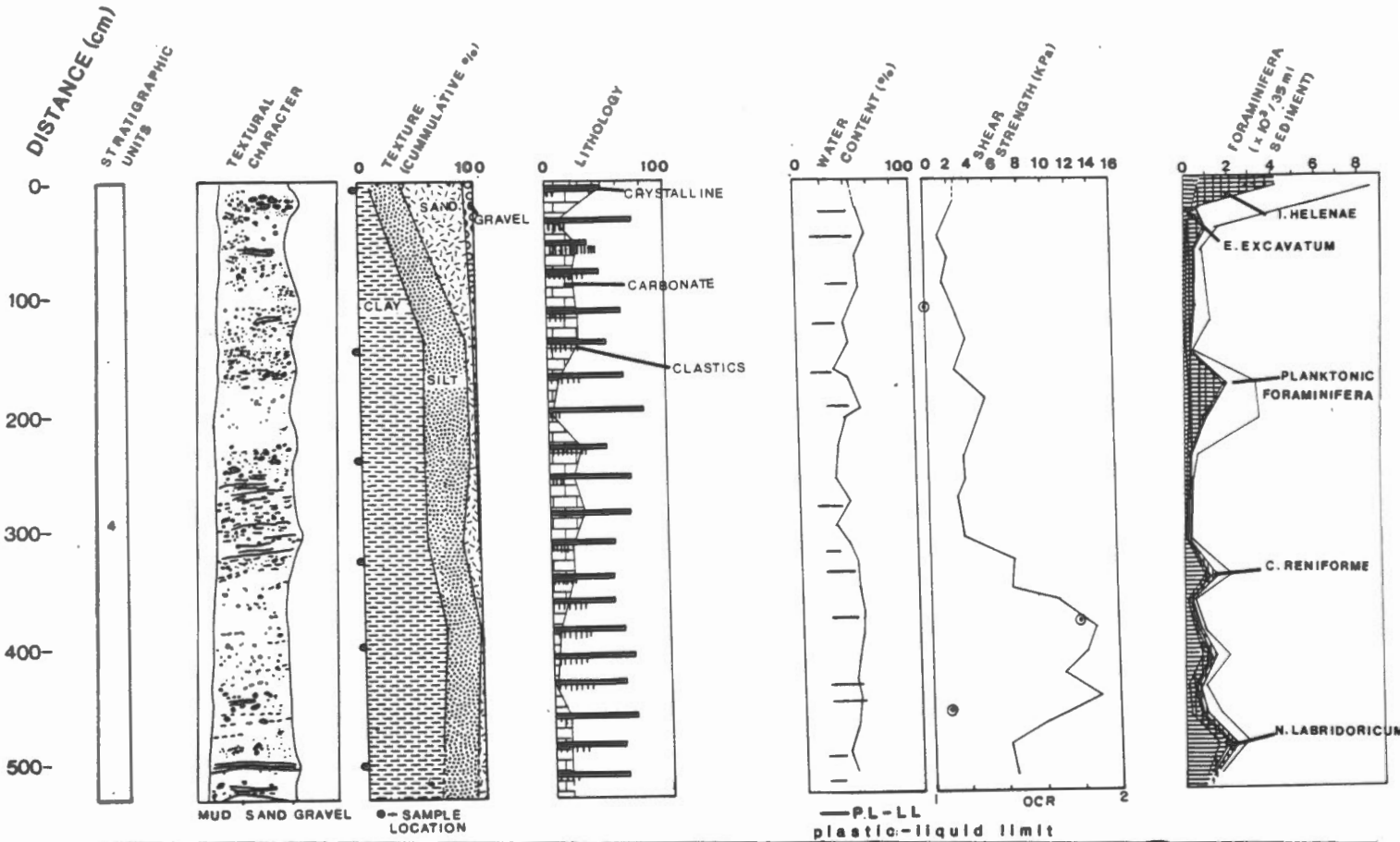


Fig. 11. Summary of properties and associated seismic section:

HU84-035-014 (adapted from Josenhans et al., 1986).

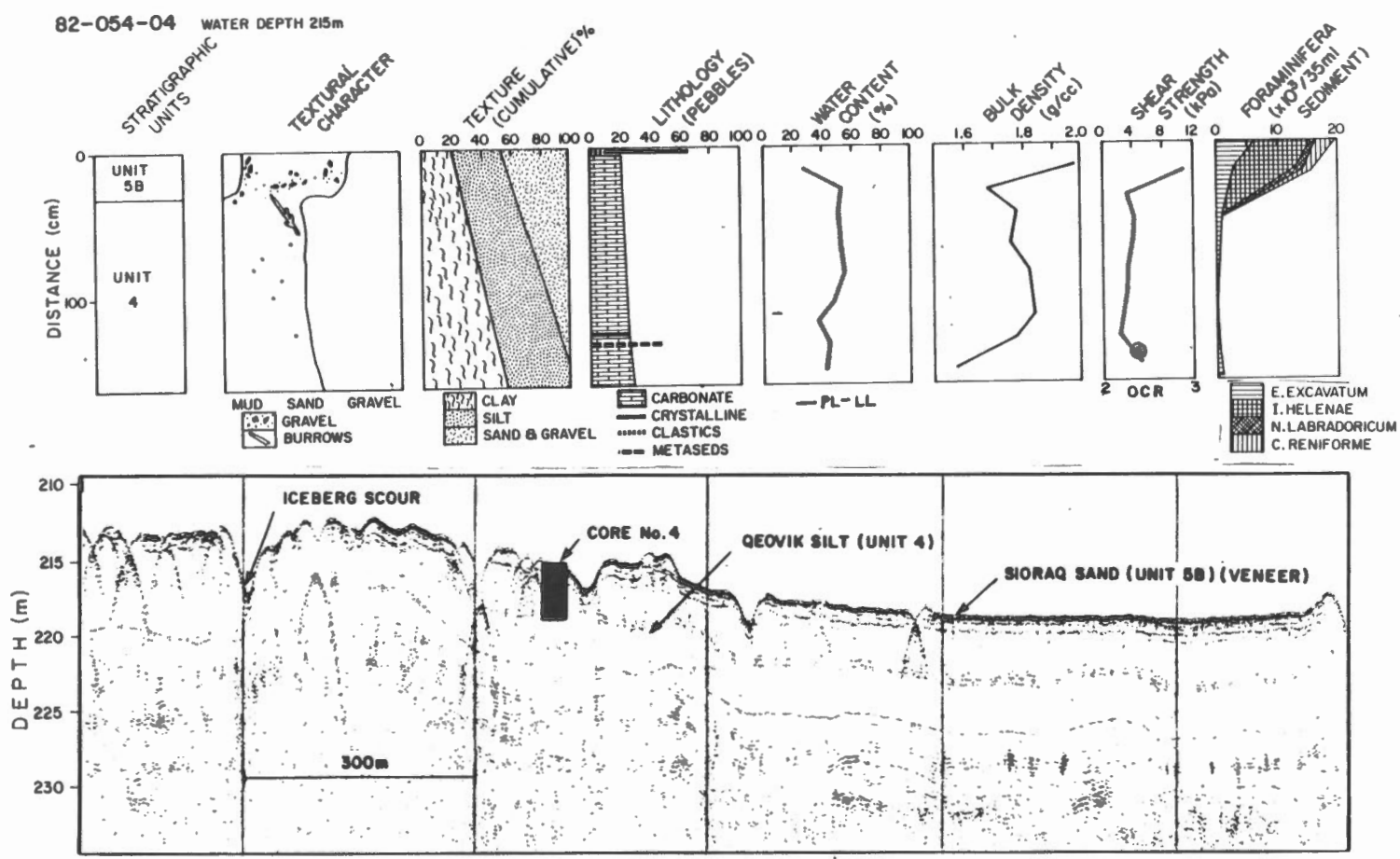


Fig. 12. Summary of properties and associated seismic section:
HU82-054-004 (adapted from Josenhans et al., 1986).

82-054-14 SEABED SLOPE 1:34 WATER DEPTH 577m

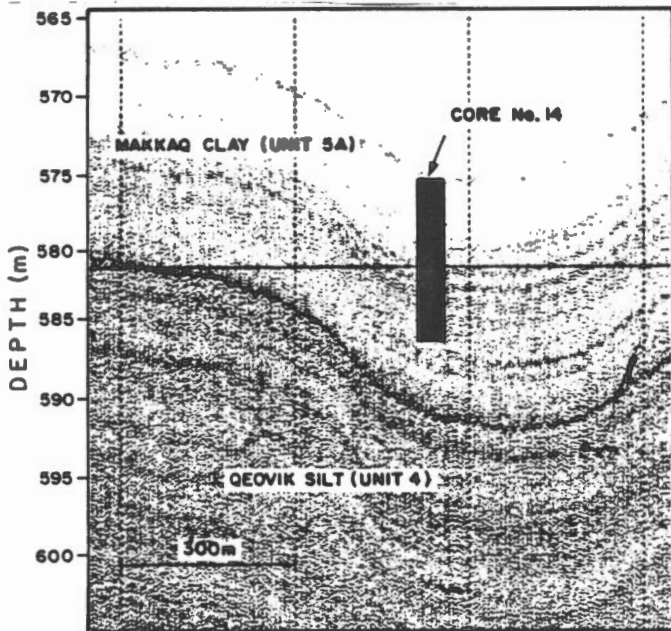
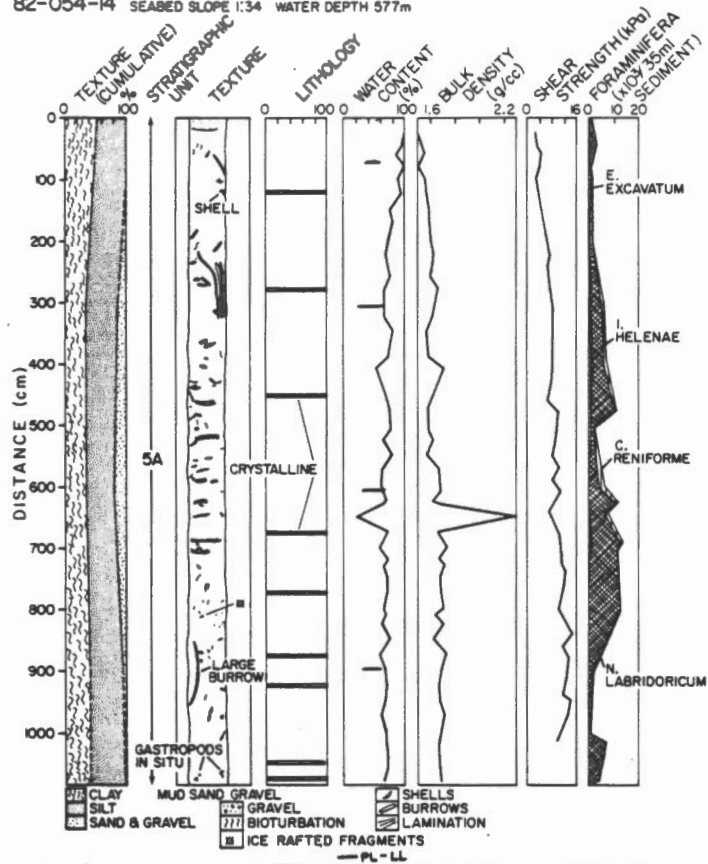


Fig. 13. Summary of properties and associated seismic section:

HU82-054-014 (adapted from Josenhans et al., 1986).

CORE 84-035-8
 WATER DEPTH: 580 M

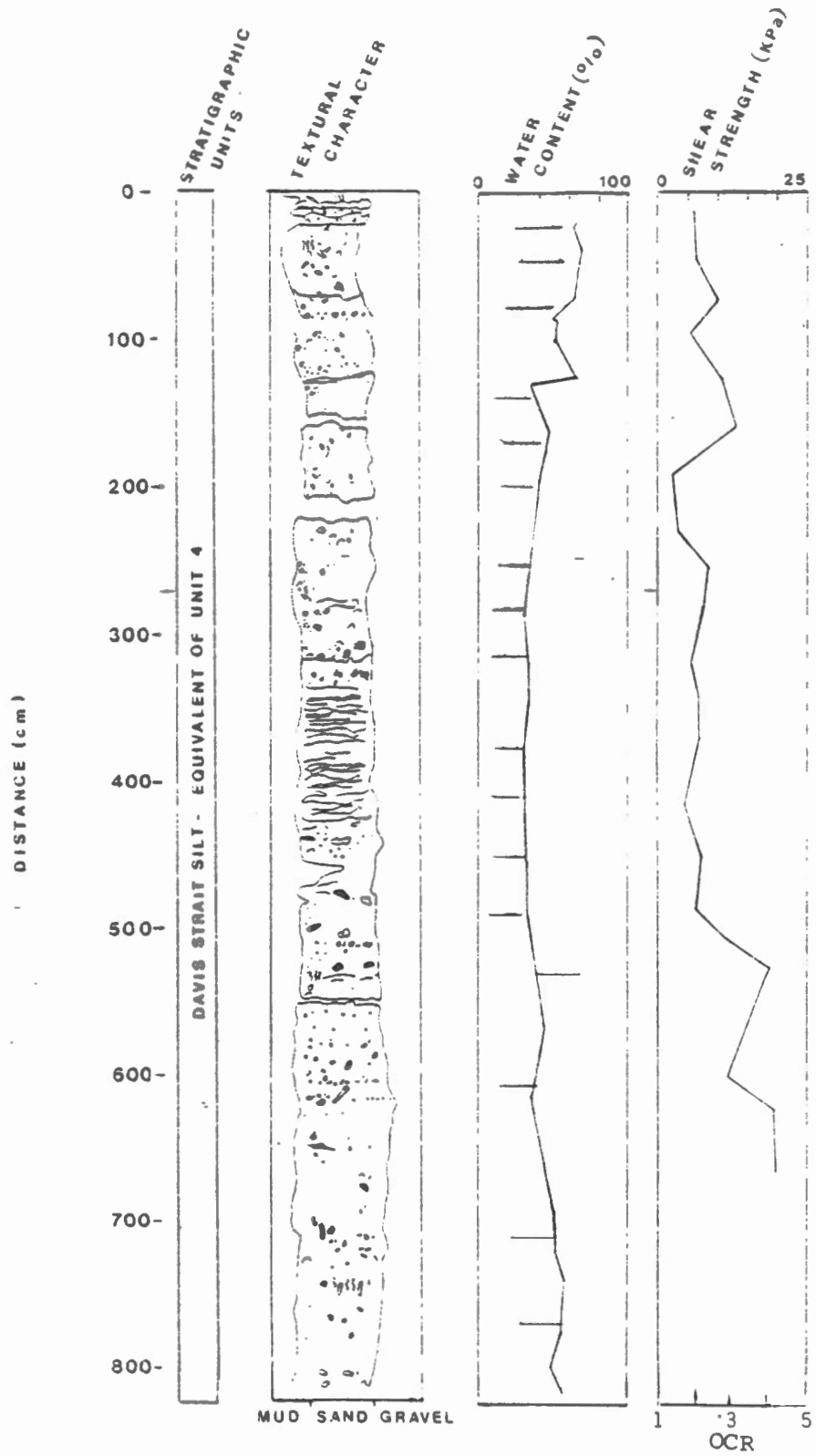


Figure 14a. Summary of properties HU84-035-008.

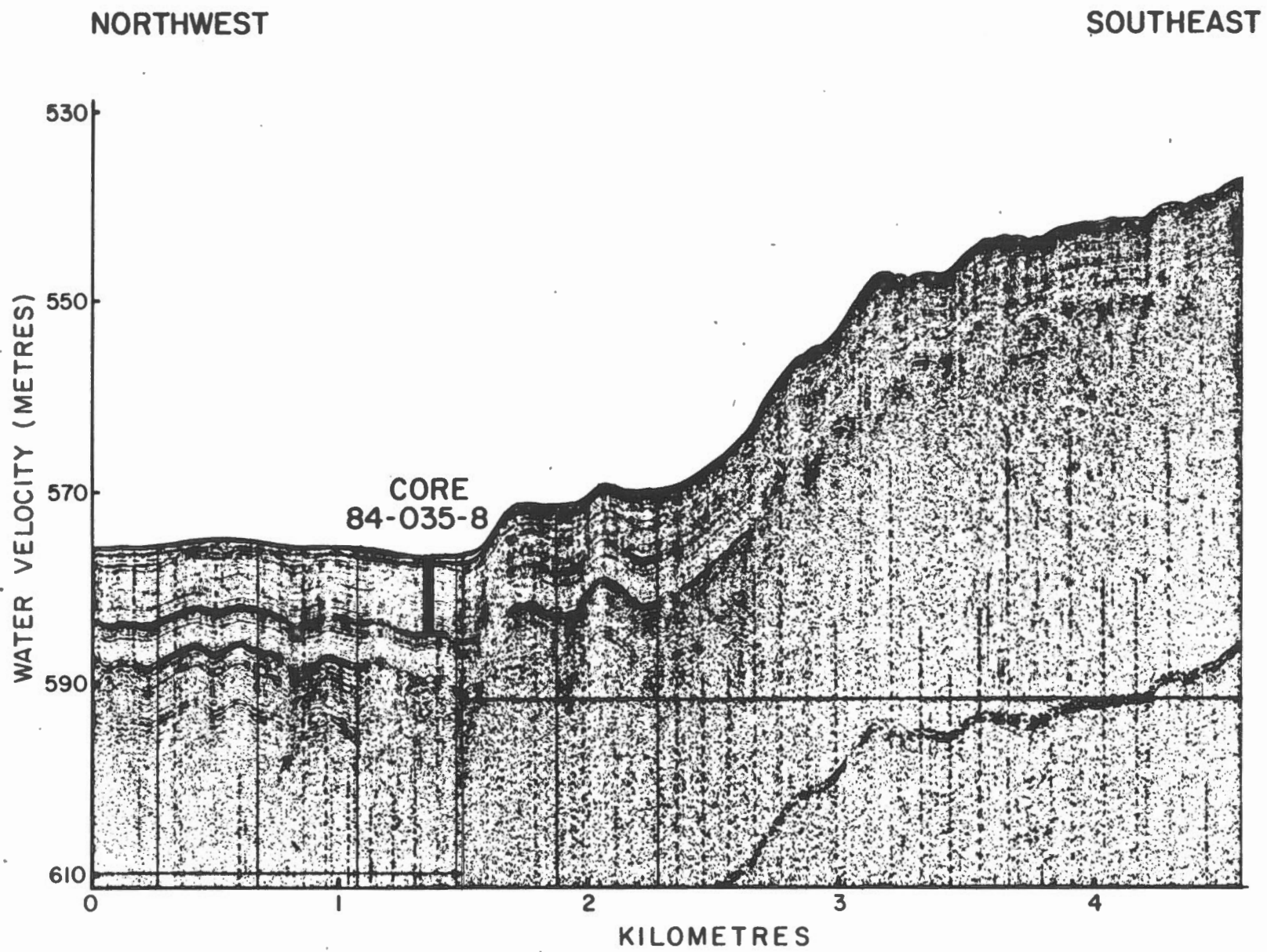


Fig. 14b. Seismic section associated with Fig. 14a (HU84-035-008).

CORE 84-035-11
WATER DEPTH: 492M

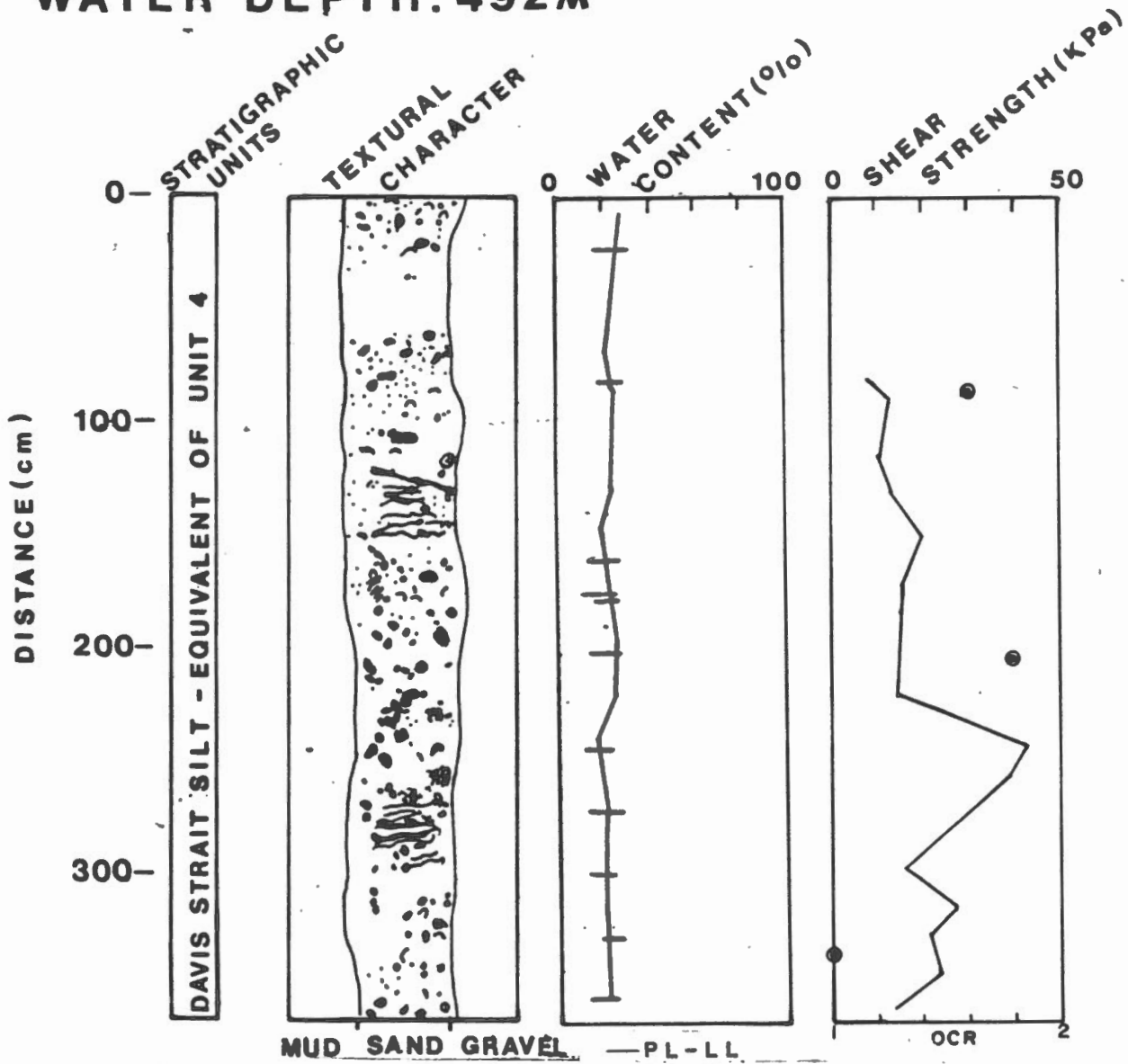


Fig. 15a. Summary of properties HU84-035-011.

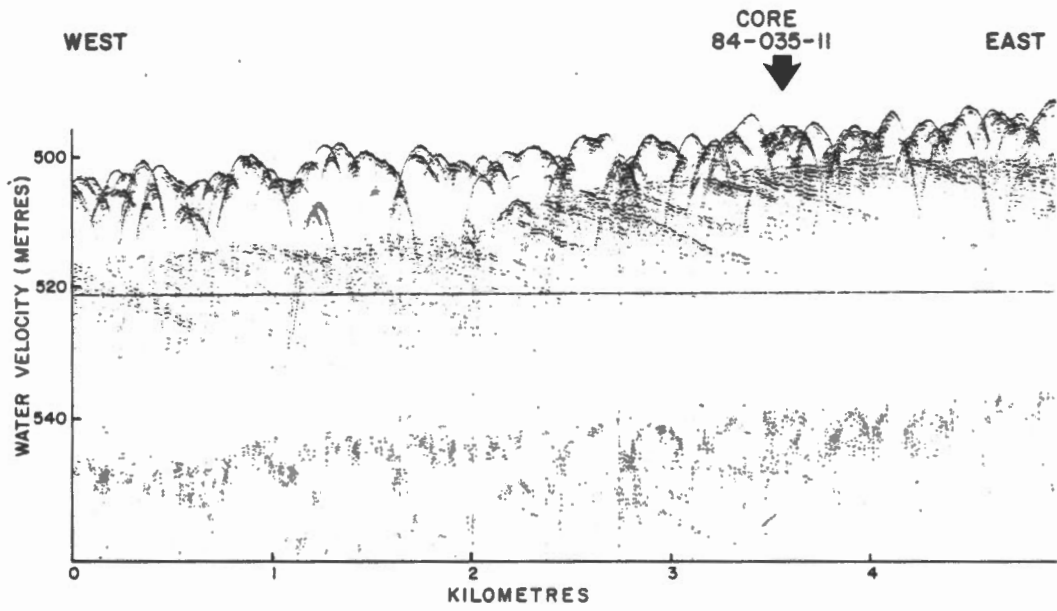


Fig. 15b. Seismic section associated with Fig. 15a (HU84-035-011).

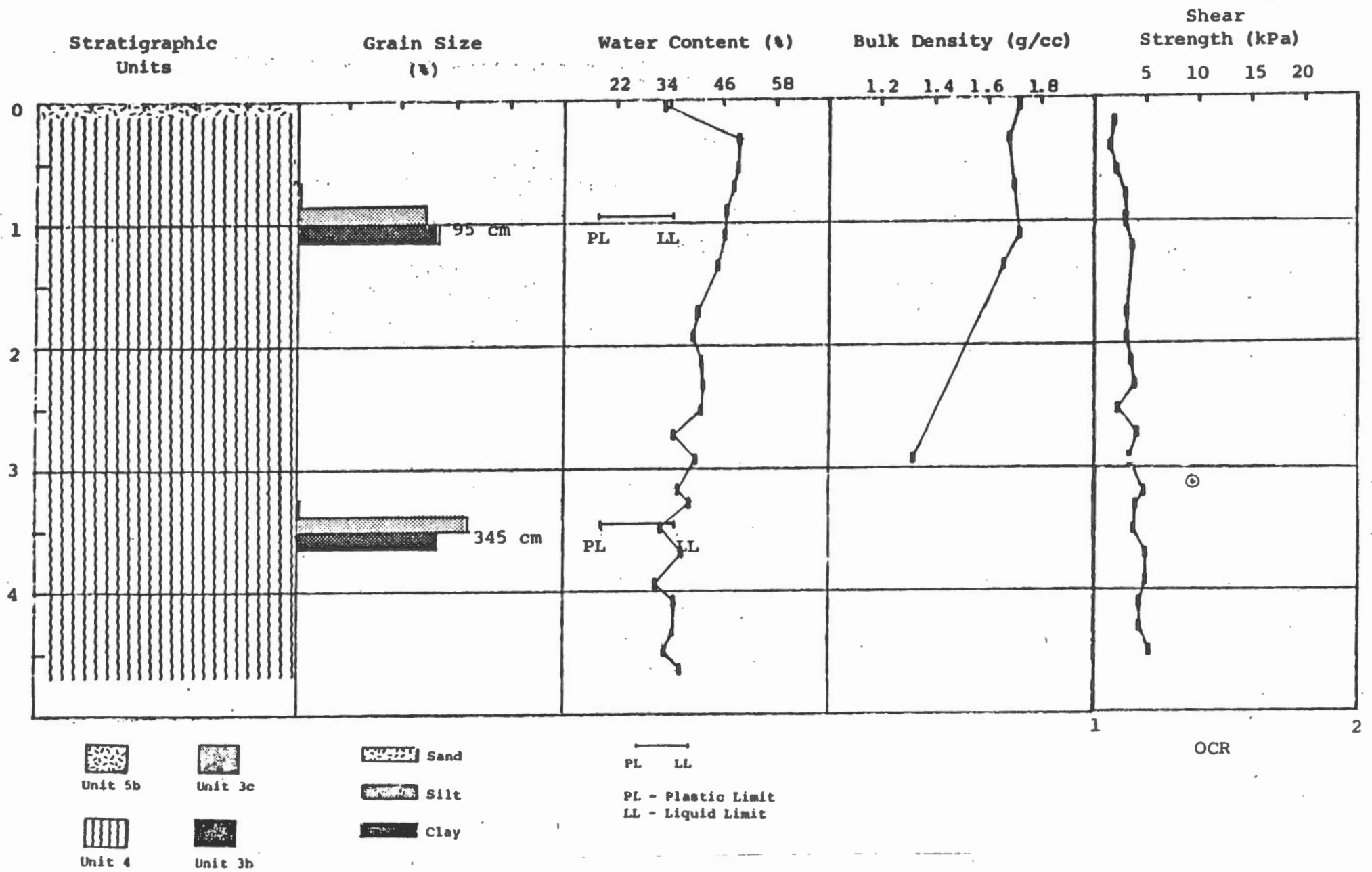


Fig. 16. Summary of properties: HU82-054-002 (from Silva et al., 1983).

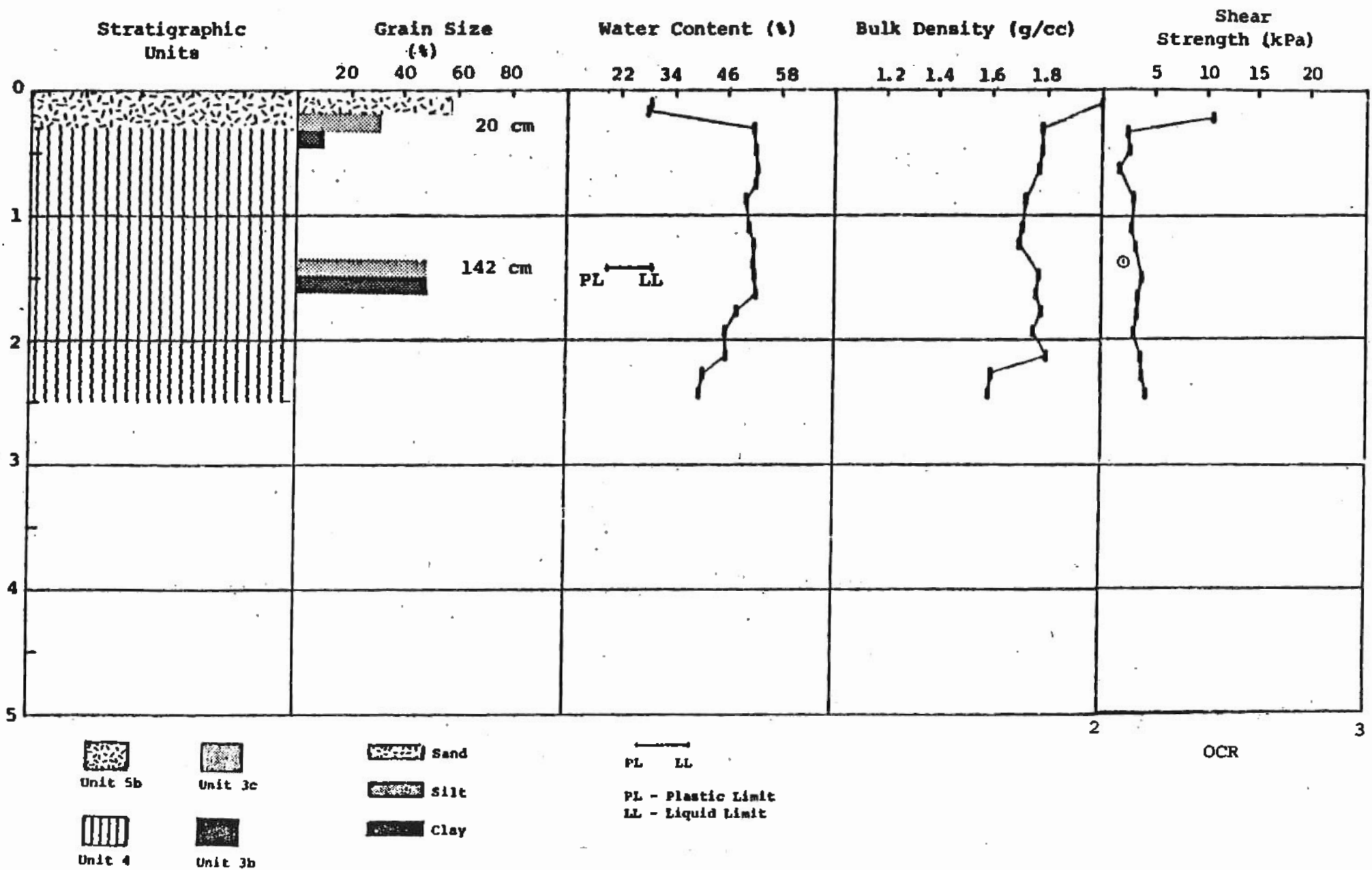


Fig. 17. Summary of properties: HU82-054-005 (from Silva et al., 1983).

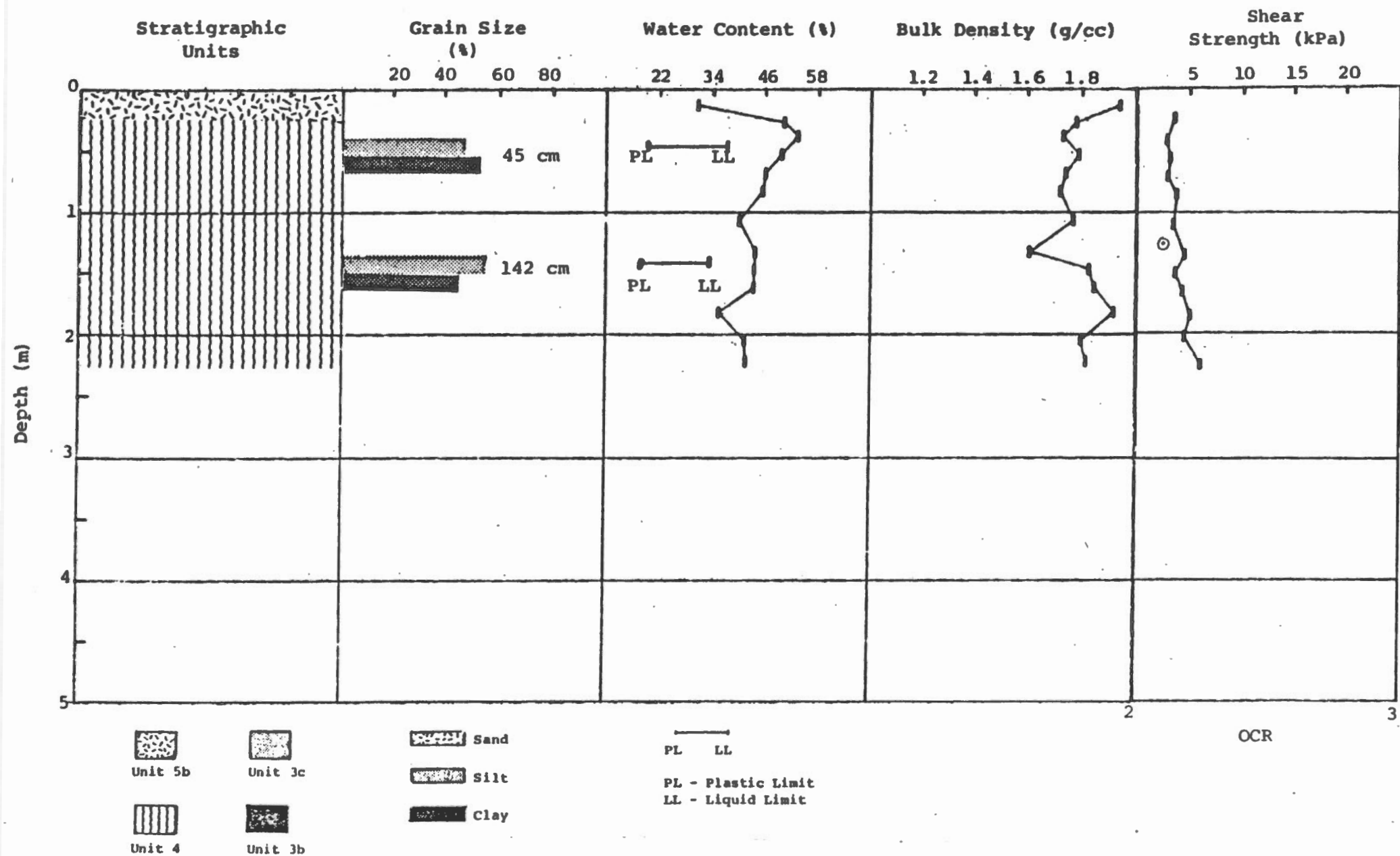
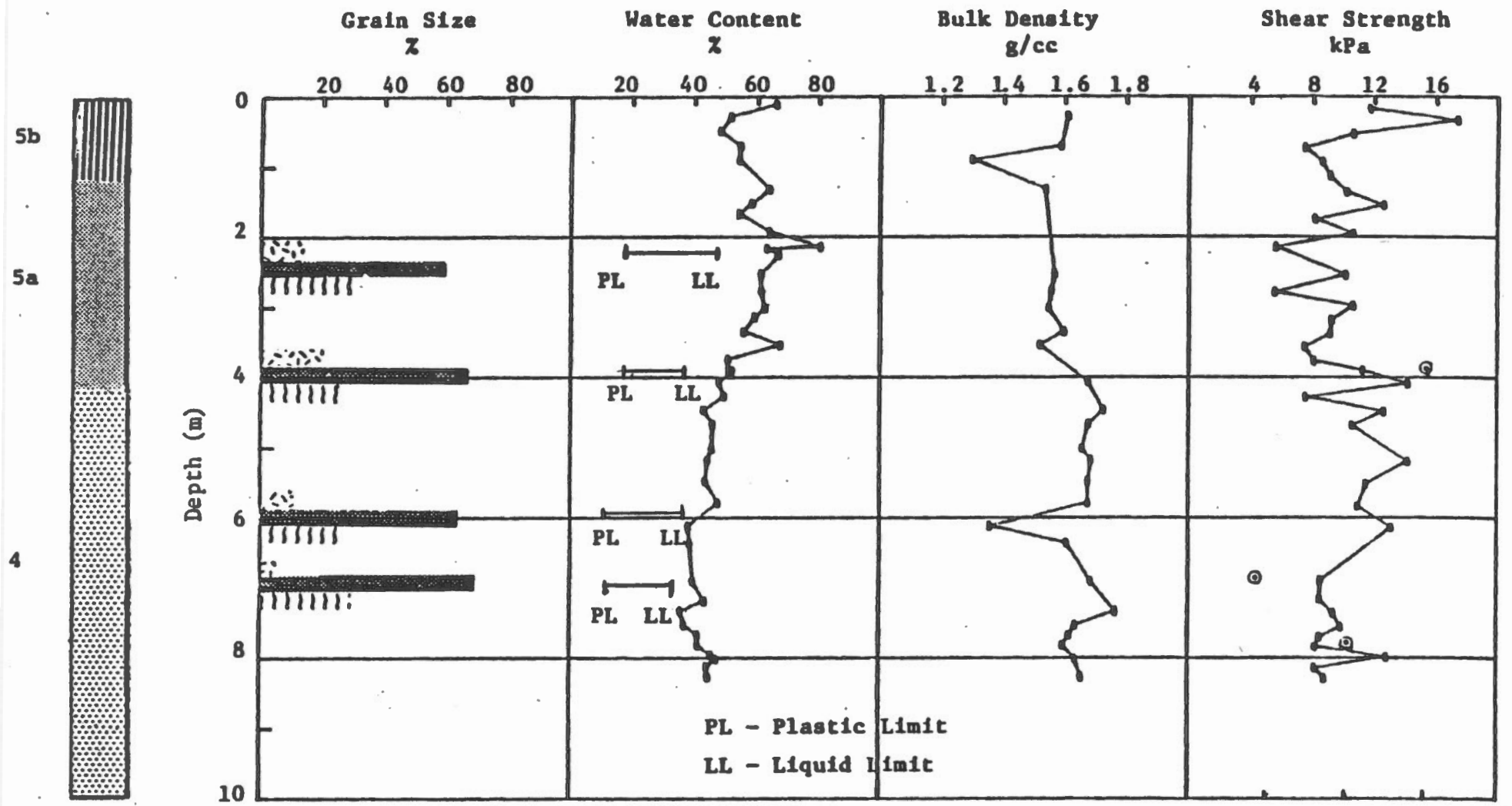


Fig. 18. Summary of properties: HU82-054-006 (from Silva et al., 1983).



LABRADOR SHELF SEDIMENTS
 PHYSICAL PROPERTY PROFILES
 HU-83-030 STA. #20

Fig. 19. Summary of properties: HU83-030-020 (from Silva et al., 1983).

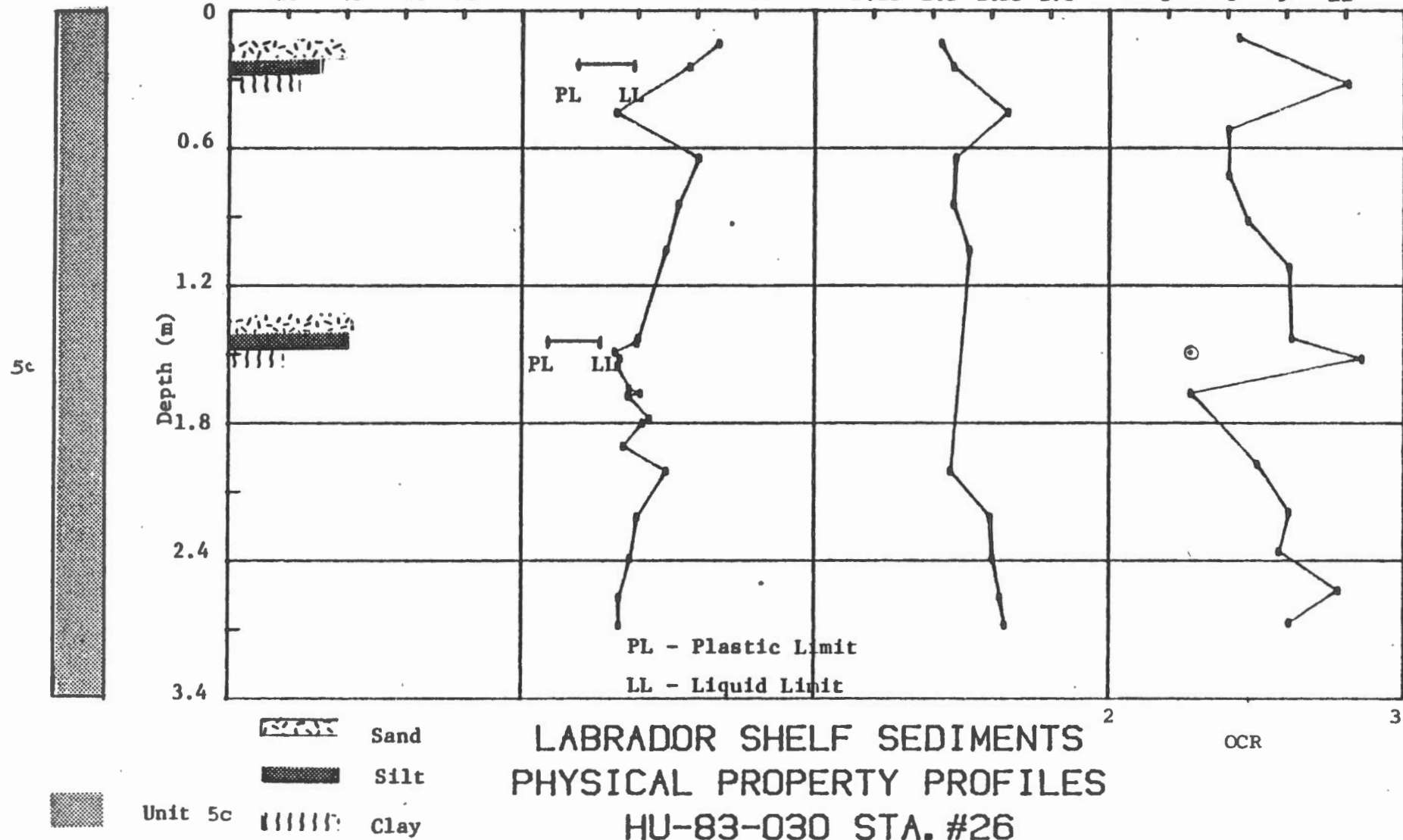
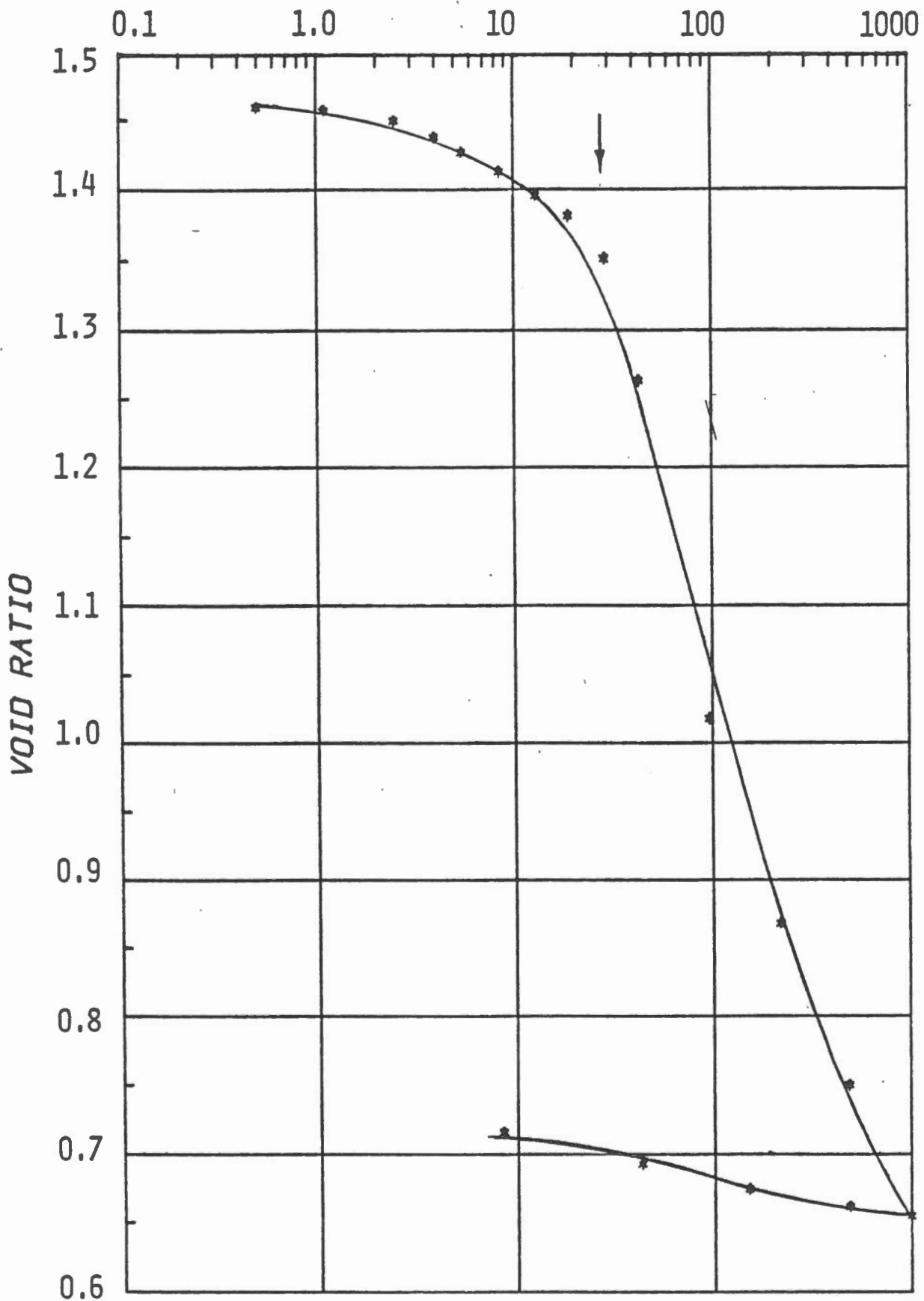


Fig. 20. Summary of properties: HU83-030-026 (from Silva et al., 1983).

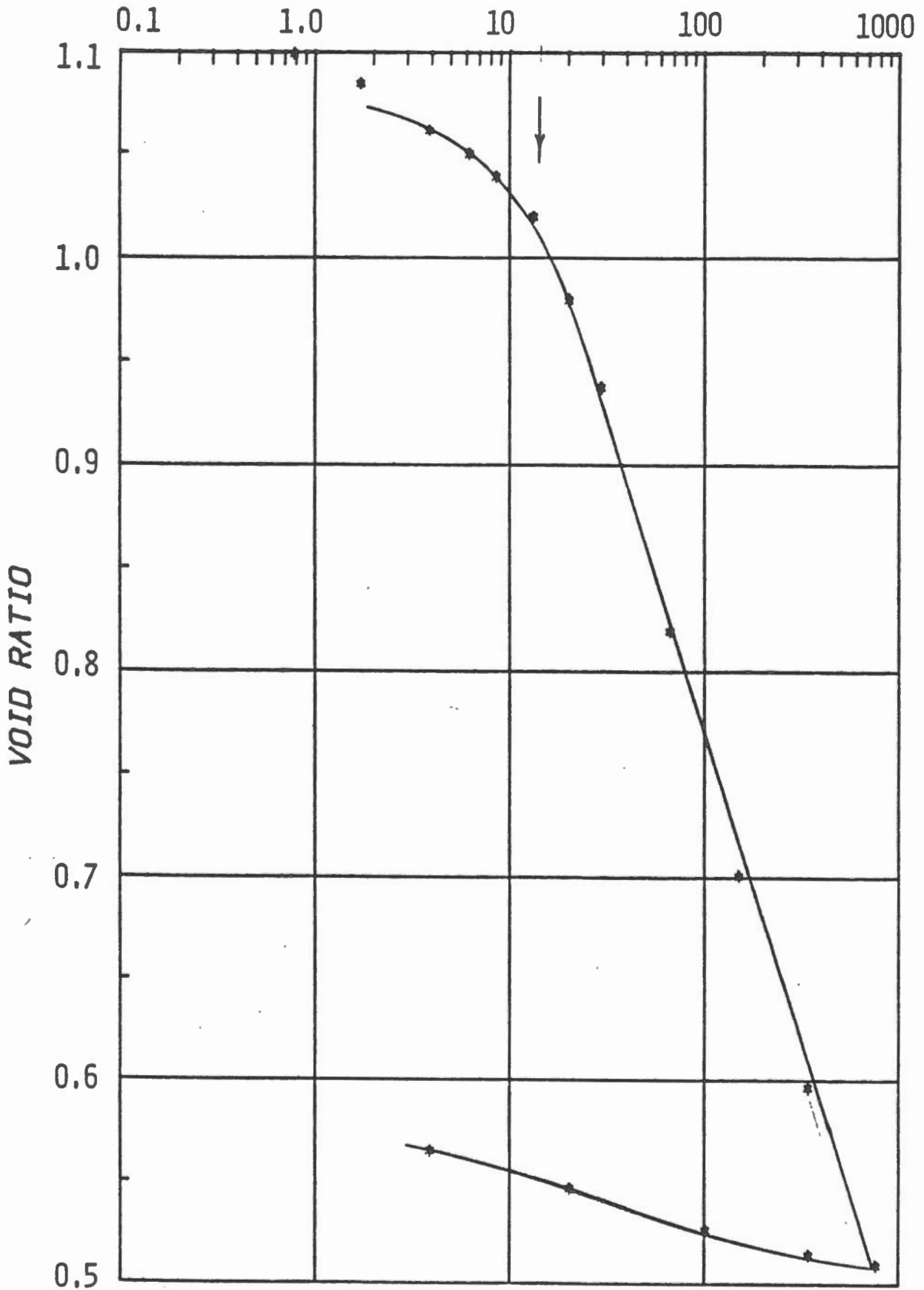
EFFECTIVE STRESS (kPa)



HU 84-035-008 87 CM

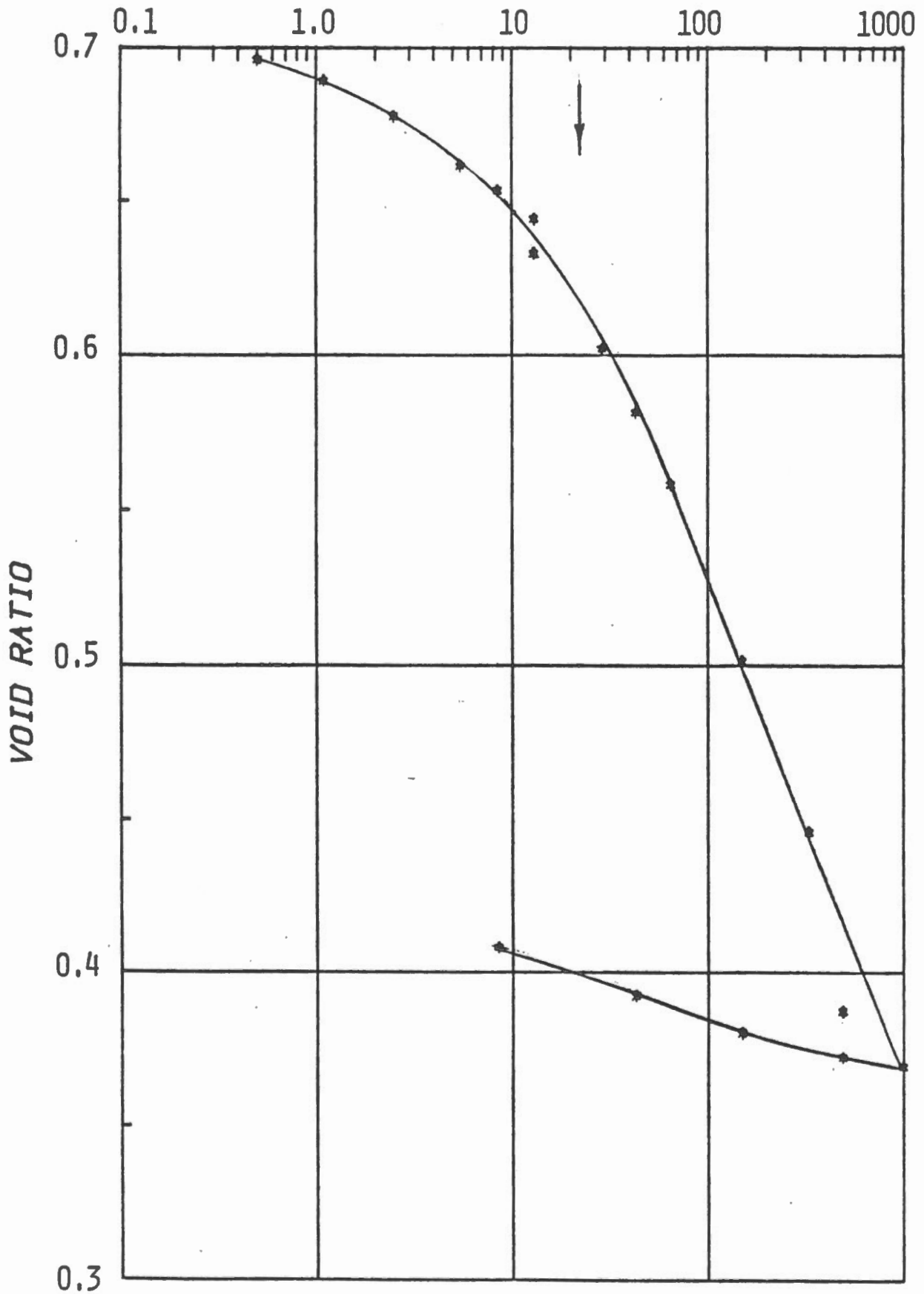
Figure B-1

EFFECTIVE STRESS (kPa)



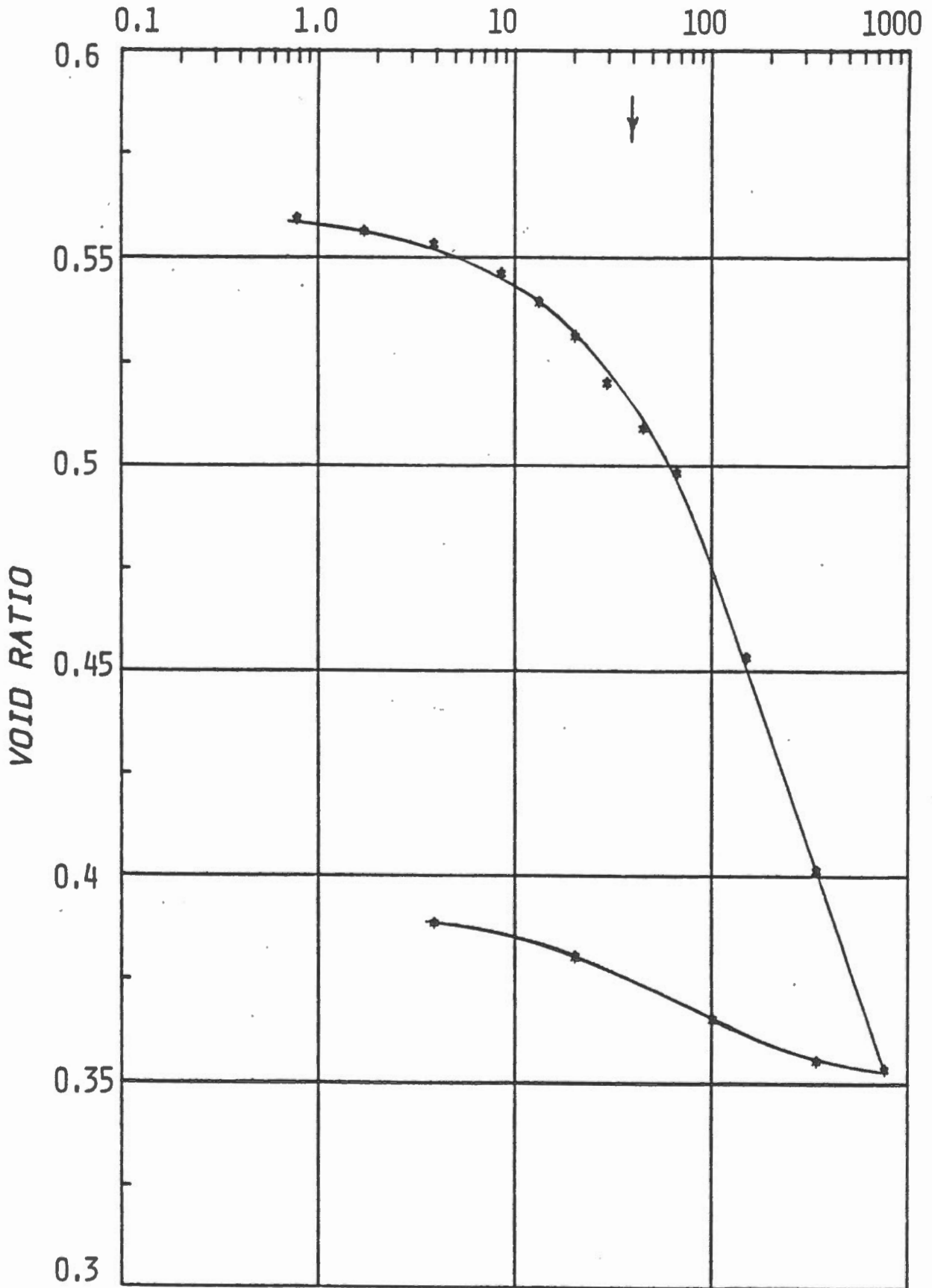
HU 84-035-008 152 CM

STRESS (kPa)

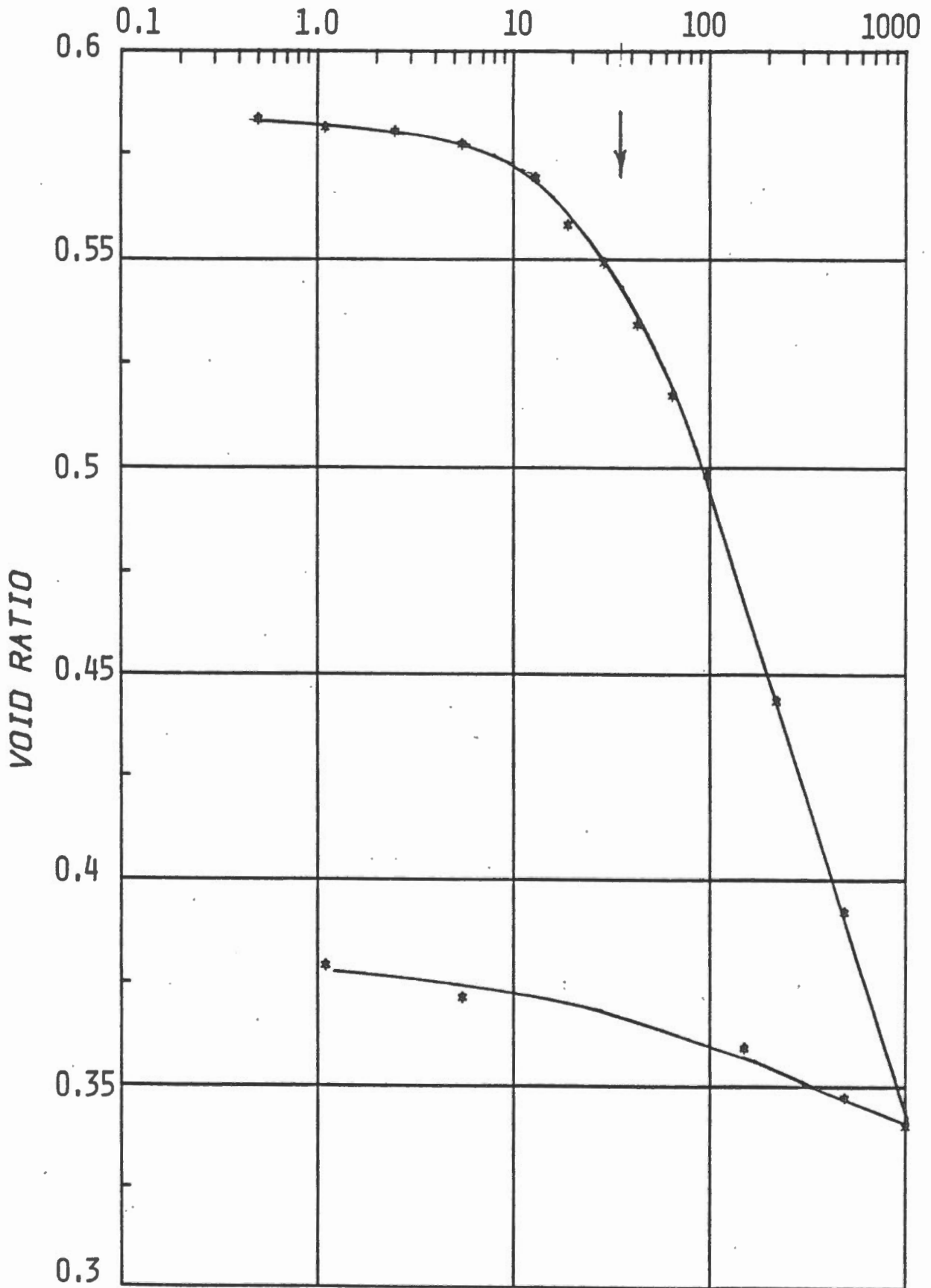


HU 84-035-011 87 CM

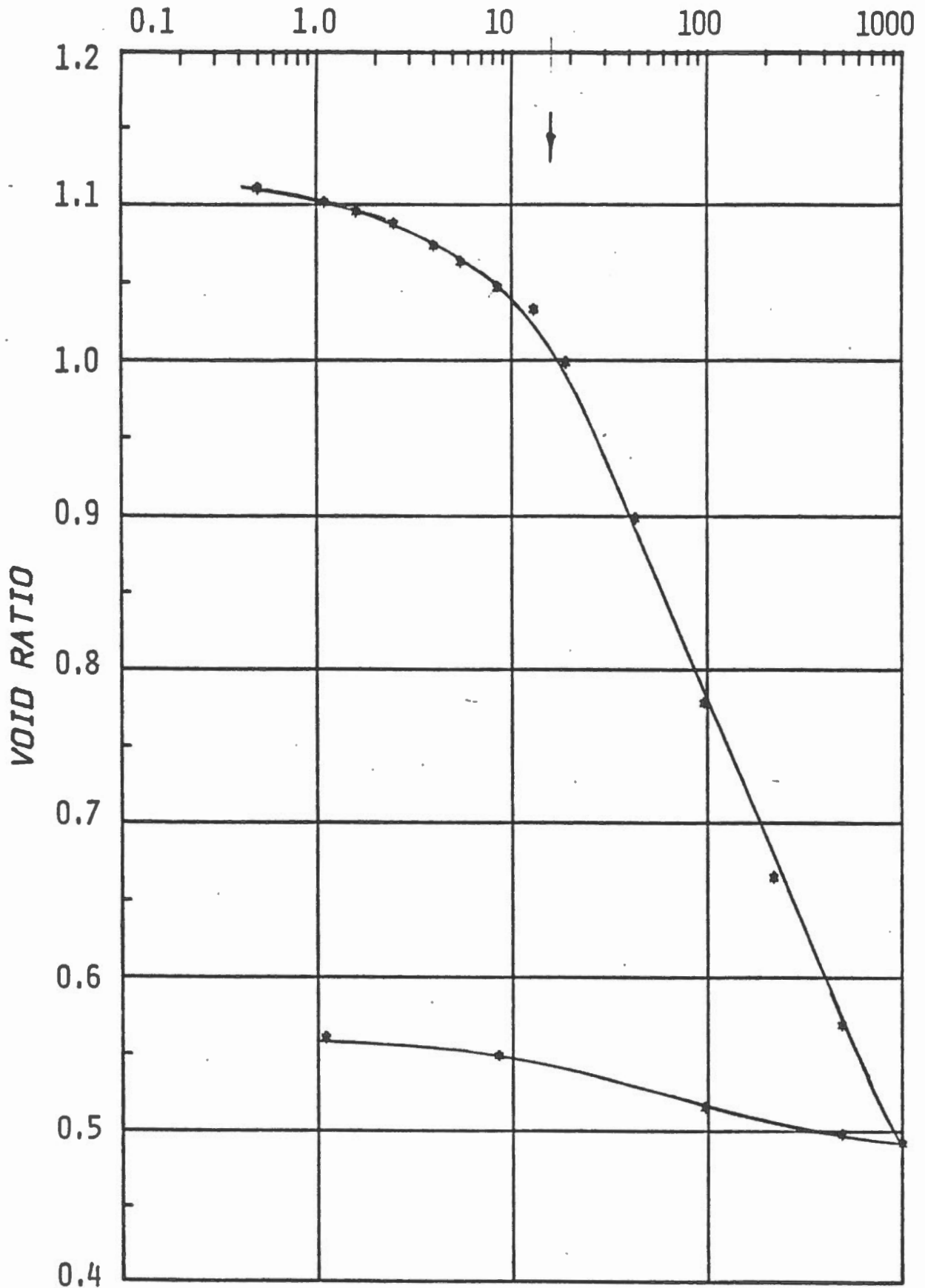
EFFECTIVE STRESS (kPa)



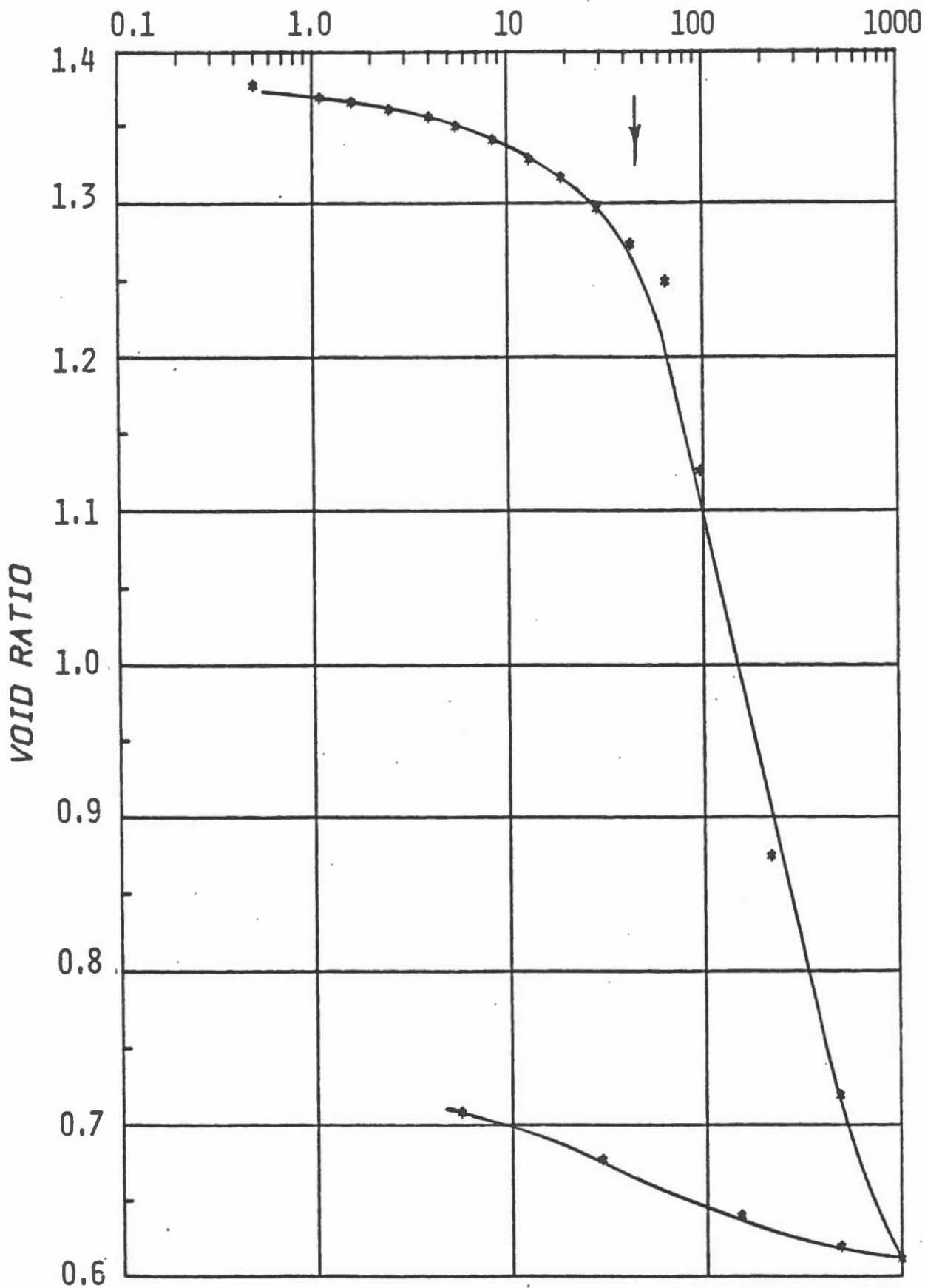
EFFECTIVE STRESS (KPA)



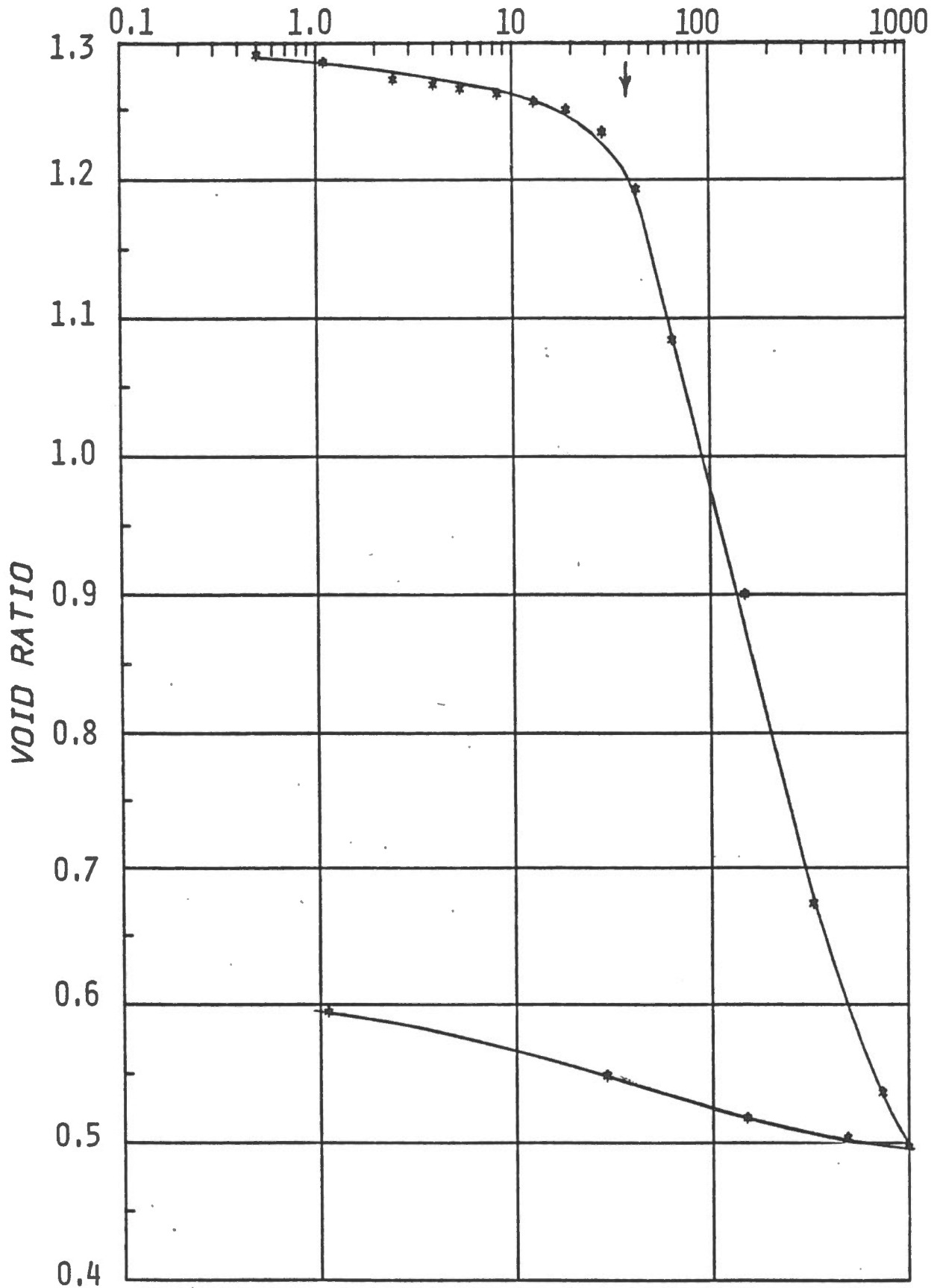
EFFECTIVE STRESS (kPa)



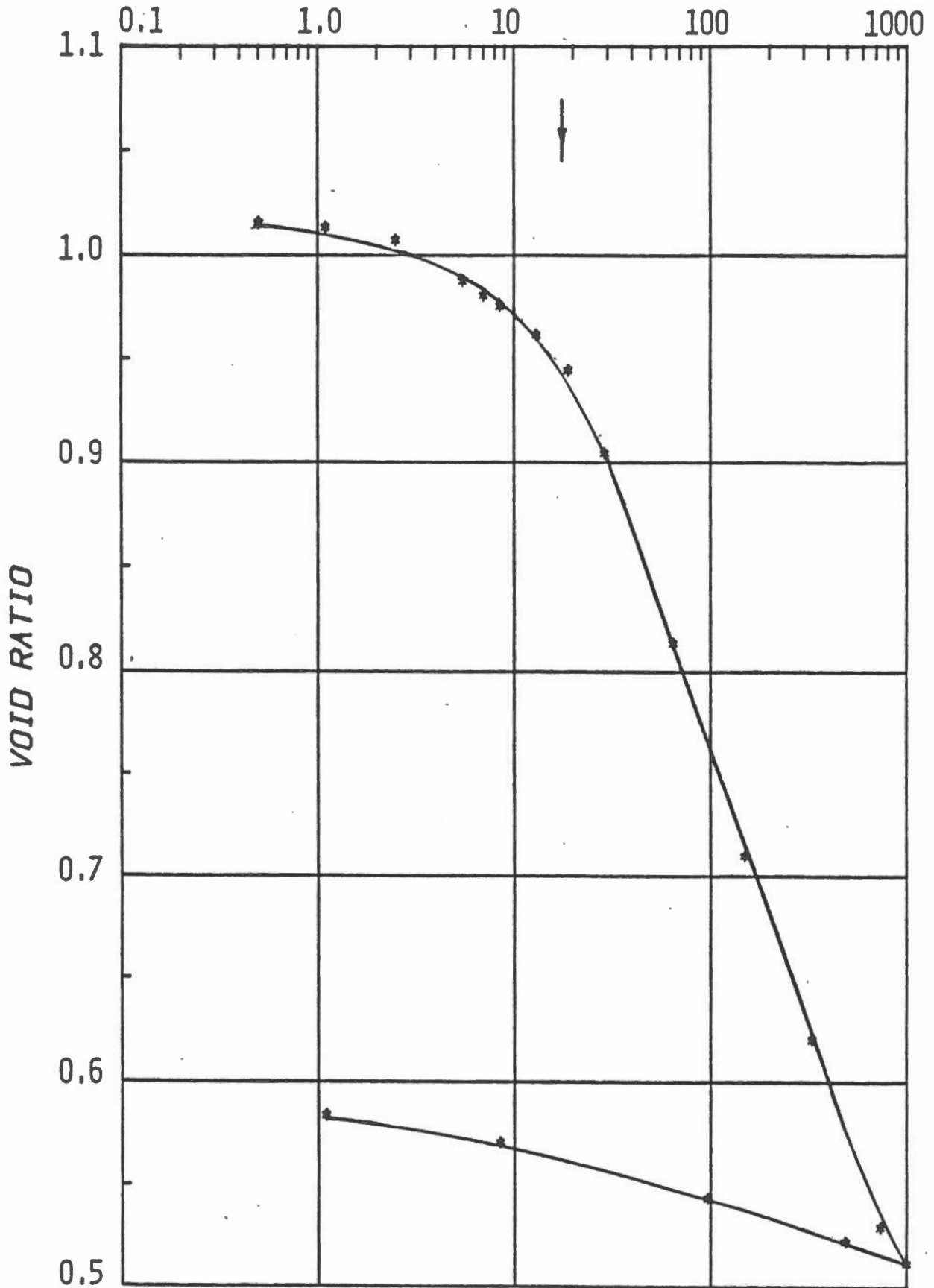
EFFECTIVE STRESS (kPa)



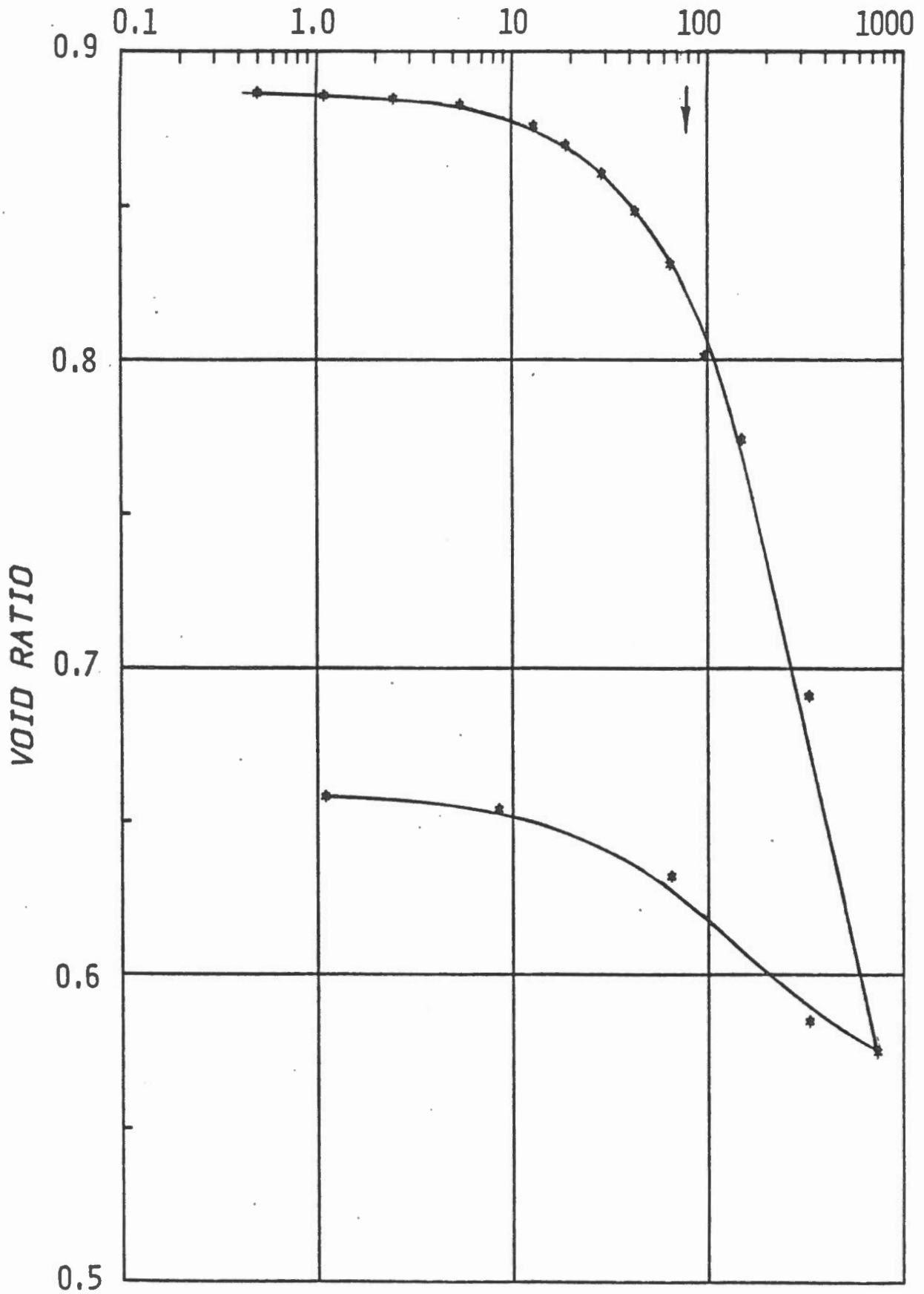
EFFECTIVE STRESS (kPa)

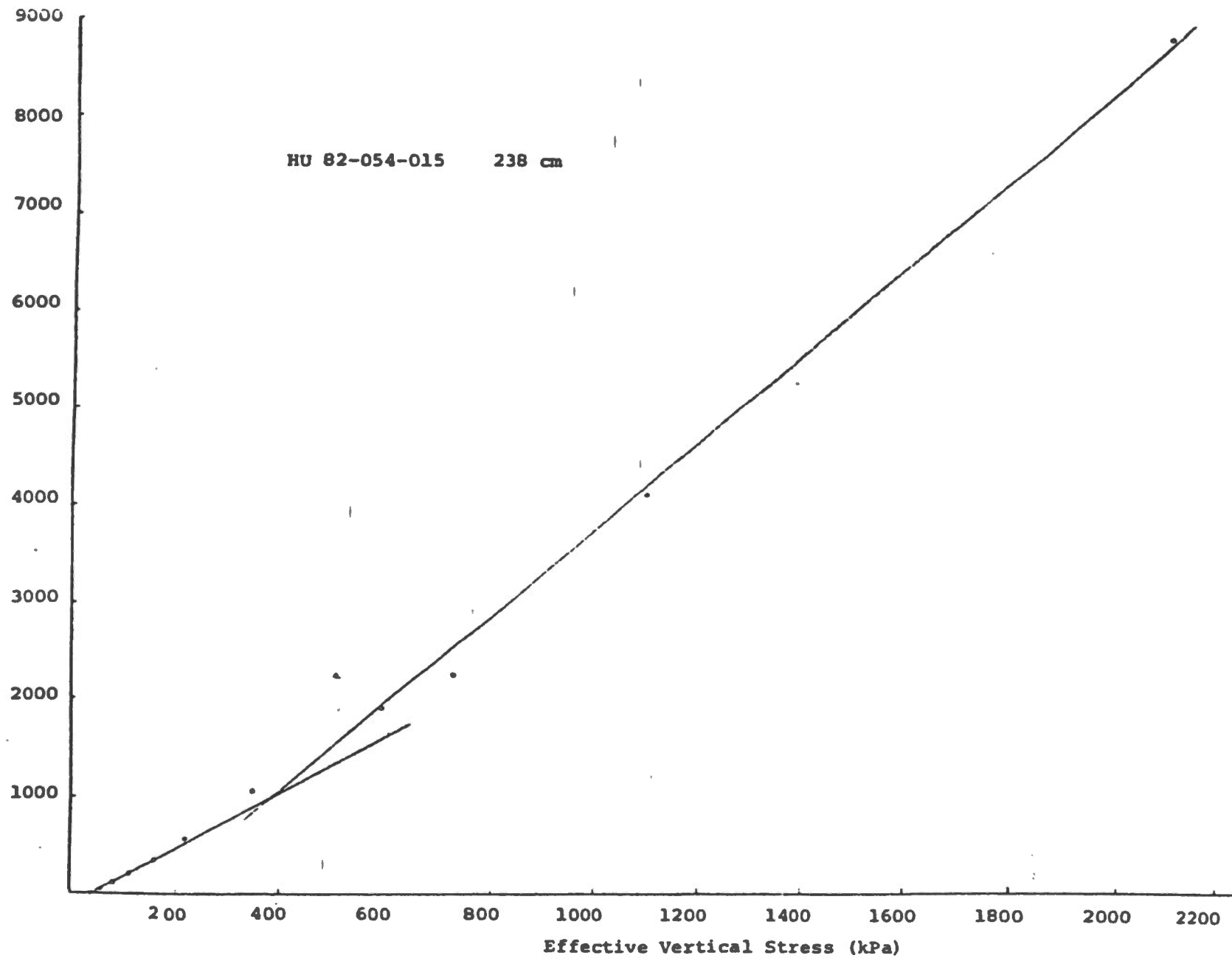


EFFECTIVE STRESS (kPa)

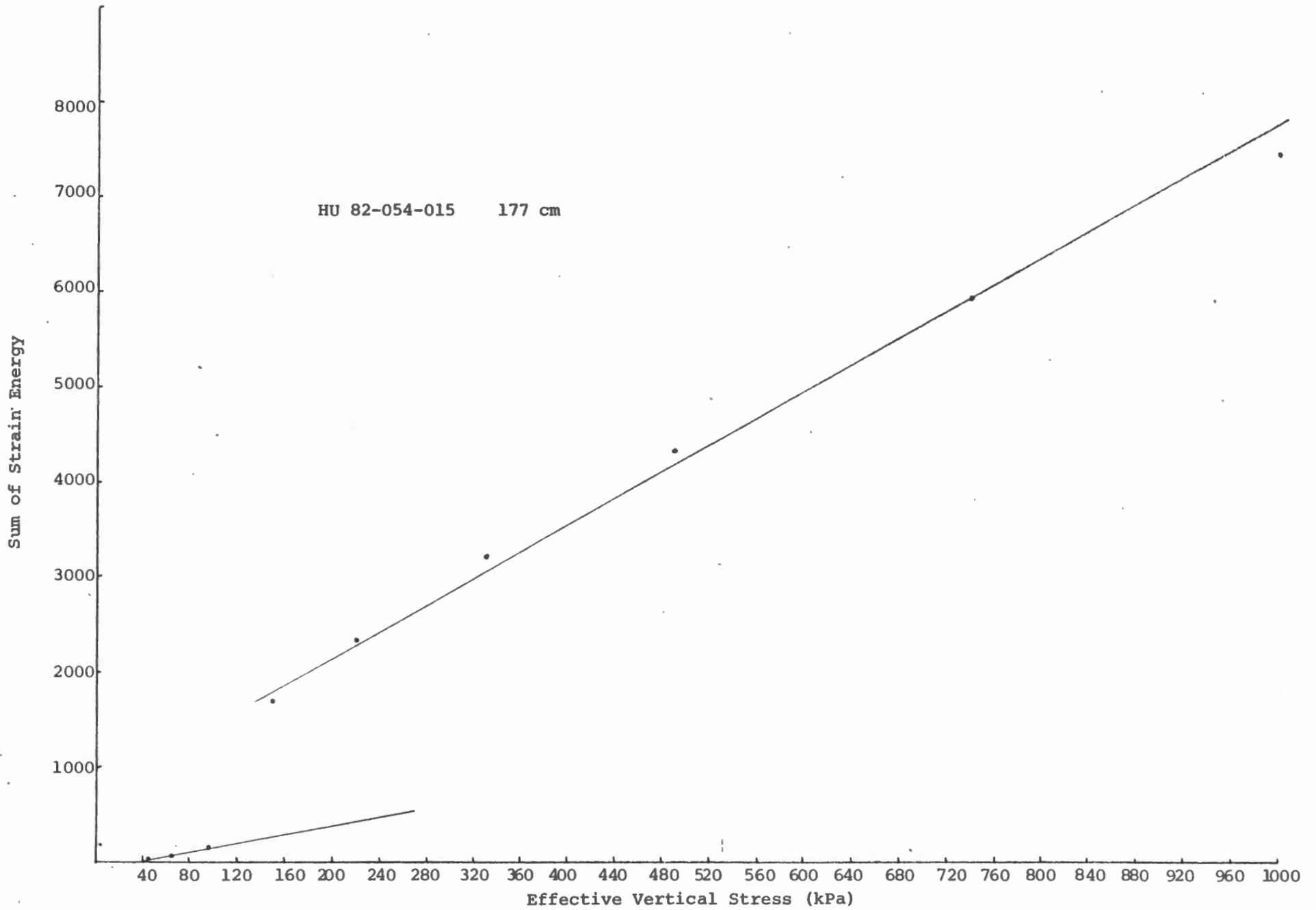


EFFECTIVE STRESS (kPa)



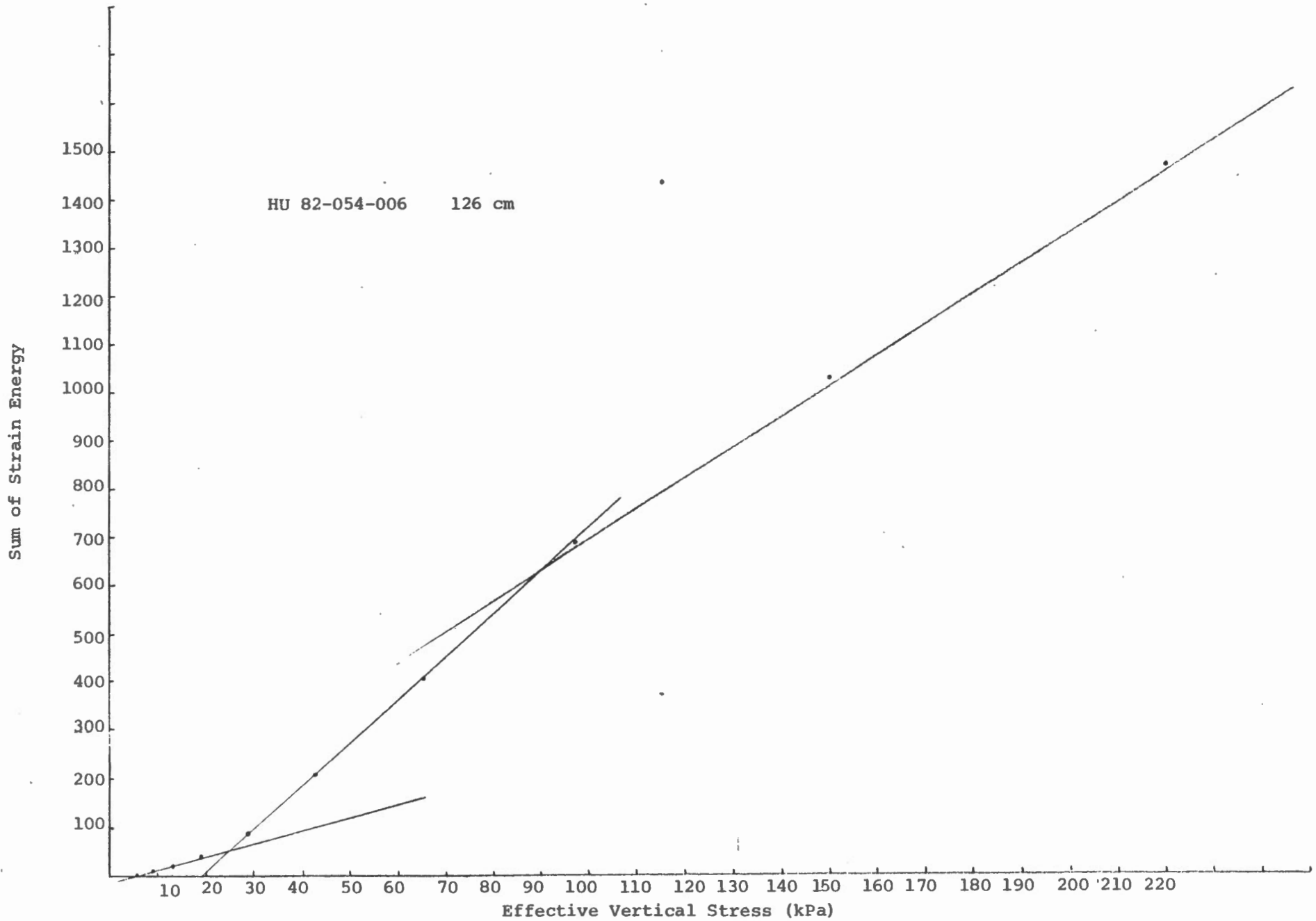


C-1. Sum of strain energy vs vertical effective stress: HU82-054-015
238 cm.



C-2 Sum of strain energy vs vertical effective stress: HU82-054-

015 177 cm.



C-3 Sum of strain energy vs vertical effective stress: HU82-054-

006 126 cm.